

**Deanship of Graduate Studies
Al-Quds University**

**Finite Volume Evolution Galerkin Schemes for Three
Dimensional Euler Equations System**

Raed Dawoud

M.Sc. Thesis

**Jerusalem-Palestine
1431/2010**

**Finite Volume Evolution Galerkin Schemes for Three
Dimensional Euler Equations System**

By

Raed Dawoud

**B.Sc.: College of Science and Technology
Al-Quds University/Palestine**

A Thesis Submitted in Partial fulfilment of Requirement for
Degree of Master of Science, Department of Mathematics
/Program of Graduate studies.

**Al-Quds University
2010**

The Program of Graduate Studies/Department of Mathematics
Deanship of Graduate Studies

**Finite Volume Evolution Galerkin Schemes for Three
Dimensional Euler Equations System**

By

Student Name: Raed Dawoud

Registration Number: 20714171

Supervisor: Dr. Yousef Zahaykah

Master thesis submitted and accepted date:

The names and signatures of the examining committee members
are as follows:

- 1- Dr. Yousef Zahaykah Head of Committe, Signature.....
- 2- Dr. Taha Abukaff Internal Examiner, Signature.....
- 3- Prof Daniel Le Roux External Examiner, Signature.....

**Al-Quds University
2010**

Declaration

I certify that the thesis, submitted for the degree of Master, is the result of my own research except where otherwise acknowledged, and that the thesis (or any part of the same) has not been submitted for a higher degree to any other university or institution.

Signed.....

Raed Dawoud

Date:

Dedication

To my mother
To the soul of my brother
To my father
To my brothers
To my sons
To my wife
To my students

Acknowledgment

This work in this thesis has been carried out at the Department of Mathematics at Al-Quds University. I cannot fully express my gratitude to my supervisor Dr. Yousef Zahaykah. He is an exceptional academic advisor, supporting, extraordinary leader and ready any time to devote his time and efforts to help his students. In the same time he set an example for me by being just, open and honest, kind and gentle person, devoted and caring constant source of wisdom and experience.

Also I would like to thank the Claude Bernard Lyon1 University in France for giving me the chance and the support to stay there four months to continue the work on my thesis under the supervision of Prof. Daniel Le Roux from the Institute of Applied Mathematics.

My gratitude also goes to Prof Le Roux for his valuable remarks which substantially improved the final product.

Also great thanks to my internal examiner Dr.Taha Abu-Kaff for his invaluable remarks.

Finally I would like to thank all the staff in the Department of mathematics at AL-Quds university.

Abstract

In this thesis we present new multidimensional schemes within the frame work of finite volume evolution Galerkin(FVEG) methods for nonlinear hyperbolic systems of conservation laws. In these schemes we couple a finite volume formulation with the approximate evolution operators, where the approximate evolution operators are constructed using the bicharacteristics of the multidimensional hyperbolic system, in which all the infinitely many directions of wave propagations are considered.

We linearize the system of Euler equations at a constant state, then we derive the exact integral representations for the three dimensional Euler equations, at this point we mimic Kirchhoff's formula that represents the solution of the wave equation and neglect the part in the integral equations that contains the integral with respect to time to obtain an approximate evolution operator, we call it N1 approximate evolution operator. We derive another approximate evolution operator by applying the midpoint rule to approximate the integral with respect to time, we call it EG3 approximate evolution operator.

The derived approximate evolution operators were used to determine the intermediate values of the Euler variables. These values determine the fluxes throughout the surfaces of each cell in the discretized domain.

Finally we used the finite volume approach to update the values of the Euler variables.

The derived FVEG schemes were applied to some numerical experiments to demonstrate the accuracy and the multidimensionality of the solution.

Contents

0	Introduction	2
1	Introductory to Euler Equations	8
2	Exact Integral Equations	13
2.1	General Theory	13
2.2	Exact Integral Equations for the Three Dimensional Euler Equations System	17
3	Evolution Galerkin Methods	35
3.1	Definition of Evolution Galerkin Schemes	35
3.2	Approximate Evolution Operators	38
3.3	Numerical Algorithms	43
3.3.1	First order algorithm for the linearized Euler equations	44
3.3.2	EG Schemes for Nonlinear Euler Equations	45
4	Numerical Experiments	48
4.1	Linearized Euler	48
4.2	Non-linear Euler	55
4.3	Conclusion and Outlook	58

Chapter 0

Introduction

The fact that certain quantities such as energy, momentum and charge are constant in physical processes has led to an increasing number of conservation laws. With the advent of quantum physics, new conserved quantities such as Baryon and Lepton numbers have been found. Certain conservation laws which lead to hyperbolic differential equations are known as hyperbolic conservation laws which govern a broad spectrum of physical phenomena in various fields e.g. material science, solid state physics, astrophysics, cosmology, fluid dynamics, atmospheric physics and multiphase flows. New problems in plasma physics, lasers and nonlinear optics created interest in the developments of the theory of nonlinear hyperbolic equations.

In recent few years major progress has been added in developing the theoretical and numerical aspects of this field. Examples of first order hyperbolic systems are wave , Maxwell and Euler equations. The solution of many hyperbolic equations contains localized phenomena. For example, sharp transition layers and discontinuities or complicated patterns in time (chaos). In such cases the exact solution is very difficult to obtain, hence a good numerical approximation is needed to resolve the discontinu-

ities efficiently. Examples of nonlinear waves are solutions to the Euler equations of gas dynamics, electromagnetic waves in nonlinear photonic crystals, dynamics of atomic lattices, surface ocean waves, light propagation along optical wave guides and traffic problems. Many numerical schemes use the finite element method (FEM) or the finite volume method (FVM) as a discrete procedure. The finite element method is mostly used for boundary value problems in the incompressible fluid flow, mechanical deformations and electromagnetic fields. The advantage of the finite element method is that it is very natural for problems that come from a variational formulation. On the other hand the FVM, based on the integral formulation of the conservation laws or other balance laws in divergence form, fulfils the discrete conservation property locally. It may also resolves discontinuities, e.g. shocks, efficiently. The FVM can discretize a domain in space using triangles, quadrilaterals or other polygons in 2D and tetrahedral, hexahedra or other polyhedral in 3D proving the FVM (like the FEM) to be a more suitable discretization technique than the finite difference method for complex geometries and unstructured grids are needed. Physical conservation laws are given by integrals over finite volumes and the FVM is based on the integral formulation of the fluxes over the boundary of the discretization cells which are called control volumes. Hence the FVM is locally. This property is very important especially in problems where fluxes are important such as fluid dynamics and heat transfer. It gives the approximate value for the derivative of a field at a given point using the values of the field at a few locations neighbouring the point. The method uses the divergence theorem, constructs a finite volume around the point, discretizes the surface bounding the volume and applies

the conservation law at each finite volume. The FVM is also a cheap and feasible method for industrial problems and can be more flexible than finite difference methods.

Many phenomena in nature which lead to multidimensional systems of hyperbolic differential equations involve infinite directions of wave propagation, hence for any numerical scheme used to solve multidimensional hyperbolic differential equations it is important to take into account the infinitely many directions of wave propagation, otherwise the solution will suffer from large discrepancies. Some of the numerical schemes exploit dimensional splitting. The splitting takes into account the mesh orientation which leads to errors in the solution. Flux vector splitting schemes (FVS) take into account wave interactions in a few directions which contribute to the numerical dissipation, see[20].

There are two main classes of finite volume schemes for the solutions of hyperbolic conservation laws: the Godunov-type upwind schemes and the central schemes. In both types of methods the approximate solution is realized by a piecewise polynomial which is reconstructed from the evolving cell-averages. Godunov's original scheme forms the basis of all upwind schemes. Its high order and multidimensional generalizations were constructed, analyzed, and implemented with great success during the 1970s and 1980s. Upwind schemes evaluate their cell-averages over the same spatial cells at all time steps. This in turn requires characteristic information along the discontinuous interfaces of these spatial cells. It is needed to trace the characteristic fans by using approximate Riemann solvers, dimensional splitting, etc... which greatly complicates the upwind algorithm, especially for more sophisticated problems. The Lax-Friedrichs (LxF) scheme is the other canonical first-order scheme, which is the basis of

all central scheme, see [21]. Like the Godunov scheme, it is based on piecewise-constant approximate solution. However, its Riemann-solver-free recipe is considerably simpler. Unfortunately, the excessive numerical viscosity in the LxF scheme yields a relatively poor resolution which seems to have delayed the development of a high-resolution central scheme, parallel to the earlier developments of high-resolution upwind schemes. The common feature of all NT(Nesayahu,H. Tadmor,E.)[22] central schemes is the evolution of cell averages over staggered cells, that is, cells which alternate every other time step. The importance of staggering is due to the fact that cell interfaces are secured in neighbourhoods around the smooth midcells of the previous time step. The main advantage is due to the replacement of costly Riemann characteristic decompositions from the upwind framework with straightforward quadratures and the dimensional splitting errors are avoided. At the same time, the use of high-order non-oscillatory piecewise polynomials, which are reconstructed from the staggered cell-averages, retain high resolution comparable with upwind results. For further study of these schemes the reader is referred to the literature, see [20, 21]

Morton et al. used the classical characteristic theory for general linear hyperbolic systems in the context of the finite element method and derived the so called Evolution Galerkin Schemes (EG) see e.g [5, 6]. These schemes belong to the category of upwind schemes and are genuinely multidimensional as they take into account infinite directions of wave propagation. They shifted the transport quantities along the bicharacteristics which were straight lines in this case and then projected on a finite element space. Ostkamp [18] extended the idea of EG schemes to the wave equation and to the nonlinear Euler equations in two

space dimensions, however her scheme involved the calculations of three-dimensional integrals which were not practically feasible especially for shallow water and Euler equations. To overcome this problem Lukacova, Morton and Warnecke [10] proposed the finite volume evolution Galerkin schemes (FVEG), namely EG1, EG2, EG3. In these methods the fluxes are evaluated at the cell interfaces by using the approximate evolution operators applied at the quadrature points. Since the approximate evolution operator involves integration around the sonic circle which constitutes the base of the characteristic cone, all the infinitely many directions of wave propagations are taken into account. These schemes are therefore regarded as truly multidimensional schemes. Another approximate evolution operator has been derived by Zahaykah which is referred to as EG4, see [19] scheme for the two and three dimensional wave equation system. This has been derived from the integral equations by neglecting higher order terms. The approximate evolution operator for the solution of the three dimensions Euler equations has been derived here. These methods and their finite volume versions were applied to the nonlinear Euler equations, as well as to the linearized Euler equations using a square mesh grid. Like central schemes, these schemes also do not need Riemann solvers. However, unlike the upwind schemes and central schemes, the flow variable distribution inside the solution element (SE) is not calculated through a reconstruction procedure using its neighbouring values at the same time level. Instead they are calculated as a part of local space-time flux conservation.

All the previous work on Euler equations was on the two dimensional case, see [8, 11, 12, 13]. The subject here is to generalize the evolution Galerkin scheme to the three dimensional

Euler equations. The aim is to construct a method that takes into account all the infinitely many directions of propagation using bicharacteristics. Numerical experiments are presented to demonstrate the accuracy and the multidimensional behaviour of the solution.

This thesis is organised as follows. We first present a general introduction. In Chapter 0 we present a small introduction about Euler equations. In Chapter 2 the general theory of bicharacteristics has been presented which we used to derive the exact integral representation of the system of Euler equations in three dimensions. In Chapter 3 we define the evolution Galerkin method and we derive the approximate evolution operators for the linearized Euler equations system, also in this chapter numerical algorithms for linearized Euler equations as well as for nonlinear Euler equations will be explained. In Chapter 4 three numerical experiments will be presented, two are based on the linearized Euler equations system. In the first one we solve the advection equation system, the second one is to simulate the propagation of an acoustic pulse, and the last one is the so-called 3d sod problem which will be solved using the nonlinear form. In the first two experiments we compare with the exact solution.

Chapter 1

Introductory to Euler Equations

A wide variety of problems in mechanics are modelled as a system of nonlinear hyperbolic conservative partial differential equations. Euler equations are a system of nonlinear hyperbolic conservation laws that govern the dynamics of a compressible material, such as gases, liquids at high pressure. Its a simpler version of the Navier-Stokes system. The latter contains terms to represent viscosity and thermal conductivity of the gas. In astrophysics these are normally not thought to be important. Using the Euler equations also implies using a fluid approximation, i.e. the particles interact with each other sufficiently to establish a Maxwell-Boltzmann distribution. This is mostly valid, but there are exceptions.

Hyperbolic equations have two important properties:

- They allow discontinuous solutions. In physical terms this means that the flow can contain shocks or contact discontinuities.

- One can define the so called characteristics or characteristic speeds. These are the eigenvalues of the problem. The solution can be written in terms of a sum of eigenvectors, three in the case of a one-dimensional problems. The three eigenvectors are so called waves and are physically associated with the characteristic speeds v , $v - s$, $v + s$, the velocity of the flow, and the velocity of the sound added and subtracted. The physical relevance is that in gas no signal can travel faster than the local speed of sound, and $|v - s|$ and $|v + s|$ are the highest possible signal speed within a flow with velocity v . This also means that the characteristics delineate a domain of influence in space-time. There is a close relation between the characteristics and the shocks, if for example an explosion occurs at a point x , its effect will spread with the characteristic speed $v - s$, $v + s$.

Definition(Conservation laws)

Conservation laws are systems of partial differential equations that are written in the form

$$\frac{\partial \mathbf{u}}{\partial t} + \sum_{j=1}^d \frac{\partial}{\partial x_j} \mathbf{f}_j(\mathbf{u}) = 0, \quad \mathbf{x} = (x_1, \dots, x_d)^T \in R^d, t > 0$$

where

$$\mathbf{u} = \begin{pmatrix} u_1 \\ \cdot \\ \cdot \\ \cdot \\ u_p \end{pmatrix},$$

is a vector valued function represents the states, and the functions

$$\mathbf{f}_j = \begin{pmatrix} f_{1j} \\ \cdot \\ \cdot \\ \cdot \\ f_{pj} \end{pmatrix},$$

are called the flux functions.

In terms of hyperbolic conservation laws Euler equations consist of three conservation laws.

Conservation of mass

$$\rho_t + (\rho u)_x = 0, \quad (1.0.1)$$

conservation of momentum

$$(\rho u)_t + (\rho u^2 + p)_x = 0, \quad (1.0.2)$$

conservation of energy

$$E_t + [(E + p)u]_x = 0. \quad (1.0.3)$$

So Euler equations in conserved variables can be expressed as,

$$\begin{bmatrix} \rho \\ \rho u \\ E \end{bmatrix}_t + \begin{bmatrix} \rho u \\ \rho u^2 + p \\ (E + P)u \end{bmatrix}_x = 0$$

where ρ is the *density*, u is the *velocity*, p is the *pressure*, and $E = \rho(\frac{1}{2}u^2 + e)$ is the *energy* with internal energy e .

In two and three space dimensions, Euler equations take the same form with ρv added to the conservation of momentum in the two space dimensions, and $\rho v, \rho w$ added in the case of three

space dimensions, where v and w are the velocities in y and z directions respectively. That is Euler equations in three space dimensions are

$$\begin{bmatrix} \rho \\ \rho u \\ \rho v \\ \rho w \\ E \end{bmatrix}_t + \begin{bmatrix} \rho u \\ \rho u^2 + p \\ \rho uv \\ \rho uw \\ (E + p)u \end{bmatrix}_x + \begin{bmatrix} \rho v \\ \rho uv \\ \rho v^2 + p \\ \rho vw \\ (E + p)v \end{bmatrix}_y + \begin{bmatrix} \rho w \\ \rho uw \\ \rho vw \\ \rho w^2 + p \\ (E + p)w \end{bmatrix}_z = 0$$

Another form that is more comprehensible physically is obtained by working with the primitive variable ρ, u and p instead of the conserved variables, since the density, velocity and pressure are more meaningful, (if we want to plot the solution of Euler equations, these variables that are plotted).

Expanding derivatives in equation (1.0.1), we obtain

$$\rho_t + u\rho_x + \rho u_x = 0. \quad (1.0.4)$$

By expanding the derivatives in the momentum equation 1.0.2, we get

$$u[\rho_t + u\rho_x + \rho u_x] + \rho[u_t + uu_x + \frac{1}{\rho}p_x] = 0. \quad (1.0.5)$$

Using 1.0.4 and then dividing through by ρ gives

$$u_t + uu_x + \frac{1}{\rho}p_x = 0. \quad (1.0.6)$$

In similar way, the energy equation (1.0.3) can be rearranged so that using (1.0.5) and (1.0.6), we can find that

$$p_t + \rho c^2 u_x + up_x = 0.$$

Thus the quasi-linear form is

$$\begin{bmatrix} \rho \\ u \\ p \end{bmatrix}_t + \begin{bmatrix} u & \rho & 0 \\ 0 & u & 1/\rho \\ 0 & \rho c^2 & u \end{bmatrix} \begin{bmatrix} \rho \\ u \\ p \end{bmatrix}_x = 0. \quad (1.0.7)$$

Similar systems can be derived for the two and three space dimensions. For two dimensions this system reads

$$\begin{bmatrix} \rho \\ u \\ v \\ p \end{bmatrix}_t + \begin{bmatrix} u & \rho & 0 & 0 \\ 0 & u & 0 & 1/\rho \\ 0 & 0 & u & 0 \\ 0 & \rho c^2 & 0 & u \end{bmatrix} \begin{bmatrix} \rho \\ u \\ v \\ p \end{bmatrix}_x \\ + \begin{bmatrix} v & 0 & \rho & 0 \\ 0 & v & 0 & 0 \\ 0 & 0 & v & 1/\rho \\ 0 & 0 & \rho c^2 & v \end{bmatrix} \begin{bmatrix} \rho \\ u \\ v \\ p \end{bmatrix}_y = 0.$$

Chapter 2

Exact Integral Equations

In this chapter we have two sections. In the first section we present the general theory of bicharacteristics for general linear hyperbolic systems while in the second section we use this general theory to derive the exact integral equations for the linearized Euler equations system in three space dimensions.

2.1 General Theory

In this section we recall the derivation of the exact integral equations for a general linear hyperbolic system using the concept of bicharacteristics. The general form of the linear hyperbolic system is given as

$$\frac{\partial \mathbf{u}}{\partial t} + \sum_{k=1}^d \mathcal{A}_k \frac{\partial \mathbf{u}}{\partial x_k} = 0, \quad \mathbf{x} = (x_1, \dots, x_d)^T \in \mathbb{R}^d \quad (2.1.1)$$

where the coefficient matrices $\mathcal{A}_k, k = 1, \dots, d$, are elements of $\mathbb{R}^{p \times p}$ and the dependent variables are $\mathbf{u} = (u_1, \dots, u_p)^T = \mathbf{u}(\mathbf{x}, t) \in \mathbb{R}^p$. Let $\mathcal{A}(\mathbf{n}) = \sum_{k=1}^d n_k \mathcal{A}_k$ be the pencil matrix,

where $\mathbf{n} = (n_1, \dots, n_d)^T$ is a directional vector in \mathbb{R}^d . The matrix $\mathcal{A}(\mathbf{n})$ has p real eigenvalues λ_k , $k = 1, \dots, p$, and p corresponding linearly independent right eigenvectors $\mathbf{r}_k = \mathbf{r}_k(\mathbf{n})$, $k = 1, \dots, p$. Let $\mathcal{R} = [\mathbf{r}_1 | \mathbf{r}_2 | \dots | \mathbf{r}_p]$ be the matrix of right eigenvectors then we can define the characteristic variable $\mathbf{w} = \mathbf{w}(\mathbf{n})$ as $\partial \mathbf{w}(\mathbf{n}) = \mathcal{R}^{-1} \partial \mathbf{u}$. Since system (2.1.1) has constant coefficient matrices \mathcal{A}_k we have $\mathbf{w} = \mathcal{R}^{-1} \mathbf{u}$ or $\mathbf{u} = \mathcal{R} \mathbf{w}$. Multiplying equation (2.1.1) by \mathcal{R}^{-1} from the left we get

$$\mathcal{R}^{-1} \frac{\partial \mathbf{u}}{\partial t} + \sum_{k=1}^d \mathcal{R}^{-1} \mathcal{A}_k \mathcal{R} \mathcal{R}^{-1} \frac{\partial \mathbf{u}}{\partial x_k} = 0. \quad (2.1.2)$$

Let $\mathcal{B}_k = \mathcal{R}^{-1} \mathcal{A}_k \mathcal{R} = (b_{ij}^k)_{i,j=1}^p$, where $k = 1, 2, \dots, d$, then the equation (2.1.2) can be rewritten in the following form

$$\frac{\partial \mathbf{w}}{\partial t} + \sum_{k=1}^d \mathcal{B}_k \frac{\partial \mathbf{w}}{\partial x_k} = 0.$$

Let us introduce the decomposition $\mathcal{B}_k = \mathcal{D}_k + \mathcal{B}'_k$, where \mathcal{D}_k contains the diagonal part of the matrix \mathcal{B}_k . This yields

$$\frac{\partial \mathbf{w}}{\partial t} + \sum_{k=1}^d \mathcal{D}_k \frac{\partial \mathbf{w}}{\partial x_k} = - \sum_{k=1}^d \mathcal{B}'_k \frac{\partial \mathbf{w}}{\partial x_k} =: \mathbf{s}. \quad (2.1.3)$$

where $\mathcal{B}'_k = (b_{ij}^k)_{i,j=1, i \neq j}^p$.

The i -th bicharacteristic corresponding to the i -th equation of (2.1.3) is defined as

$$\frac{d\mathbf{x}_i}{dt} = \mathbf{b}_{ii}(\mathbf{n}) = (b_{ii}^1, b_{ii}^2, \dots, b_{ii}^d)^T,$$

where $i = 1, \dots, p$. Here b_{ii}^k are the diagonal entries of the matrix \mathcal{B}_k , $k = 1, \dots, d$, $i = 1, \dots, p$.

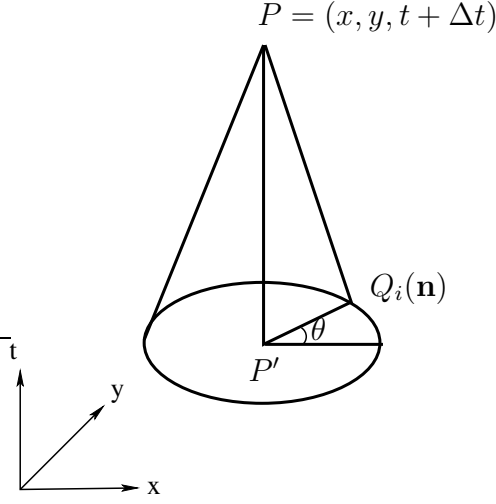


Figure 2.1: Bicharacteristics along the Mach cone through P and $Q_i(\mathbf{n})$, $d = 2$.

We consider the bicharacteristics backwards in time. Therefore the initial conditions are $\mathbf{x}_i(t + \Delta t, \mathbf{n}) = \mathbf{x}$ for all $\mathbf{w} \in \mathbb{R}^d$ and $i = 1, \dots, p$, i.e. $\mathbf{x}_i(\tilde{t}, \mathbf{n}) = \mathbf{x} - \mathbf{b}_{ii}(\mathbf{n})(t + \Delta t - \tilde{t})$. Now integration of the i -th equation of the system (2.1.3) from the point P down to the point $Q_i(\mathbf{n})$, where the bicharacteristic hits the basic plane of the characteristic cone, see Figure 2.1. Note that bicharacteristics are straight lines because the system is linear with constant coefficients. Now the i -th equation becomes

$$\frac{\partial w_i}{\partial t} + \sum_{k=1}^d b_{ii}^k \frac{\partial w_i}{\partial x_k} = - \left(\sum_{j=1, i \neq j}^d \left(b_{ij}^1 \frac{\partial w_j}{\partial x_1} + b_{ij}^2 \frac{\partial w_j}{\partial x_2} + \dots + b_{ij}^d \frac{\partial w_j}{\partial x_d} \right) \right) = s_i, \quad (2.1.4)$$

where

$$P \equiv (\mathbf{x}, t + \Delta t) \in \mathbb{R}^p \times \mathbb{R}_+$$

is taken to be a fixed point, while

$$Q_i(\mathbf{n}) = (\mathbf{x} - \Delta t \mathbf{b}_{ii}, t).$$

Taking a vector

$$\sigma_i = (b_{ii}^1, b_{ii}^2, \dots, b_{ii}^d, 1),$$

we can define the directional derivative

$$\frac{dw_i}{d\sigma_i} = \left(\frac{\partial w_i}{\partial x_1}, \frac{\partial w_i}{\partial x_2}, \dots, \frac{\partial w_i}{\partial x_d}, \frac{\partial w_i}{\partial t} \right) \cdot \sigma_i = \frac{\partial w_i}{\partial t} + b_{ii}^1 \frac{\partial w_i}{\partial x_1} + b_{ii}^2 \frac{\partial w_i}{\partial x_2} + \dots + b_{ii}^d \frac{\partial w_i}{\partial x_d}.$$

Hence the i -th equation (2.1.4) can be rewritten as follows:

$$\frac{dw_i}{d\sigma_i} = s_i = - \sum_{j=1, i \neq j}^d \left(b_{ij}^1 \frac{\partial w_j}{\partial x_1} + b_{ij}^2 \frac{\partial w_j}{\partial x_2} + \dots + b_{ij}^d \frac{\partial w_j}{\partial x_d} \right).$$

Now integration from P to $Q_i(\mathbf{n})$ gives

$$w_i(P) - w_i(Q_i(\mathbf{n}), \mathbf{n}) = s'_i, \quad i = 1, \dots, d. \quad (2.1.5)$$

where

$$s'_i = \int_t^{t+\Delta t} s_i(\mathbf{x}_i(\tilde{t}, \mathbf{n}), \tilde{t}) d\tilde{t} = \int_0^{\Delta t} s_i(\mathbf{x}_i(\tau, \mathbf{n}), t + \Delta t - \tau) d\tau.$$

Multiplication of equation (2.1.5) by \mathcal{R} from the left and $(d-1)$ -dimensional integration of the variable \mathbf{n} over the unit sphere O in \mathbb{R}^d leads to the exact integral equations for (2.1.1)

$$\mathbf{u}(P) = \mathbf{u}(\mathbf{x}, t + \Delta t) = \frac{1}{|O|} \int_O \mathcal{R}(\mathbf{n})(w_1, \dots, w_p)^T dO + \tilde{\mathbf{s}}, \quad (2.1.6)$$

where

$$w_i = w_i(Q_i(n), n) \quad i = 1, \dots, p$$

and

$$\begin{aligned}\tilde{\mathbf{s}} &= (\tilde{s}_1, \tilde{s}_2, \dots, \tilde{s}_p)^T = \frac{1}{|O|} \int_O \mathcal{R}(\mathbf{n}) \mathbf{s}' dO \\ &= \frac{1}{|O|} \int_O \int_0^{\Delta t} \mathcal{R}(\mathbf{n}) \mathbf{s}(\mathbf{x}_i(\tau, \mathbf{n}), t + \Delta t - \tau) d\tau dO\end{aligned}$$

and $|O|$ corresponds to the measure of the domain of integration.

2.2 Exact Integral Equations for the Three Dimensional Euler Equations System

In this section we will use the general theory of bicharacteristics of linear hyperbolic system to derive the exact integral equations of the three dimensional Euler equation.

Consider Euler equations system written in primitive variables

$$\mathbf{U}_t + \mathcal{A}_1(\mathbf{U})\mathbf{U}_x + \mathcal{A}_2(\mathbf{U})\mathbf{U}_y + \mathcal{A}_3(\mathbf{U})\mathbf{U}_z = 0, \quad (2.2.7)$$

$\mathbf{x} = (x, y, z)^T \in \mathbb{R}^3$, where

$$\mathbf{U} := \begin{pmatrix} \rho \\ u \\ v \\ w \\ p \end{pmatrix},$$

$$\mathcal{A}_1 := \begin{pmatrix} u & \rho & 0 & 0 & 0 \\ 0 & u & 0 & 0 & \frac{1}{\rho} \\ 0 & 0 & u & 0 & 0 \\ 0 & 0 & 0 & u & 0 \\ 0 & \rho c^2 & 0 & 0 & u \end{pmatrix},$$

$$\mathcal{A}_2 := \begin{pmatrix} v & 0 & \rho & 0 & 0 \\ 0 & v & 0 & 0 & 0 \\ 0 & 0 & v & 0 & \frac{1}{\rho} \\ 0 & 0 & 0 & v & 0 \\ 0 & 0 & \rho c^2 & 0 & v \end{pmatrix}$$

and

$$\mathcal{A}_3 := \begin{pmatrix} w & 0 & 0 & \rho & 0 \\ 0 & w & 0 & 0 & 0 \\ 0 & 0 & w & 0 & 0 \\ 0 & 0 & 0 & w & \frac{1}{\rho} \\ 0 & 0 & 0 & \rho c^2 & w \end{pmatrix}.$$

Here ρ indicates the density, u , v and w are the components of the velocity in x , y and z directions respectively, p denotes the pressure, and γ is isotropic exponent ($\gamma = 1.4$ for dry air). To derive the integral equations we linearize the system(2.2.7) by freezing the Jacobian matrices at a constant state $\mathbf{U}' = (\rho', u', v', w', p')^T$. Let c' be the local speed of sound there, i.e $c' = \sqrt{\frac{\gamma p'}{\rho}}$, then the linearized Euler equations system with frozen constant coefficients well be in the form

$$\mathbf{U}_t + \mathcal{A}_1(\mathbf{U}')\mathbf{U}_x + \mathcal{A}_2(\mathbf{U}')\mathbf{U}_y + \mathcal{A}_3(\mathbf{U}')\mathbf{U}_z = 0 \quad (2.2.8)$$

where

$$\mathbf{U} := \begin{pmatrix} \rho \\ u \\ v \\ w \\ p \end{pmatrix},$$

$$\mathcal{A}_1 := \begin{pmatrix} u' & \rho' & 0 & 0 & 0 \\ 0 & u' & 0 & 0 & \frac{1}{\rho'} \\ 0 & 0 & u' & 0 & 0 \\ 0 & 0 & 0 & u' & 0 \\ 0 & \rho'c'^2 & 0 & 0 & u' \end{pmatrix},$$

$$\mathcal{A}_2 := \begin{pmatrix} v' & 0 & \rho' & 0 & 0 \\ 0 & v' & 0 & 0 & 0 \\ 0 & 0 & v' & 0 & \frac{1}{\rho'} \\ 0 & 0 & 0 & v' & 0 \\ 0 & 0 & \rho'c'^2 & 0 & v' \end{pmatrix}$$

and

$$\mathcal{A}_3 := \begin{pmatrix} w' & 0 & 0 & \rho & 0 \\ 0 & w' & 0 & 0 & 0 \\ 0 & 0 & w' & 0 & 0 \\ 0 & 0 & 0 & w' & \frac{1}{\rho} \\ 0 & 0 & 0 & \rho'c'^2 & w' \end{pmatrix}.$$

The eigenvalues of the pencil matrix

$$\mathcal{A}(\mathbf{U}') = \mathcal{A}_1(\mathbf{U}')n_1 + \mathcal{A}_2(\mathbf{U}')n_2 + \mathcal{A}_3(\mathbf{U}')n_3 \quad (2.2.9)$$

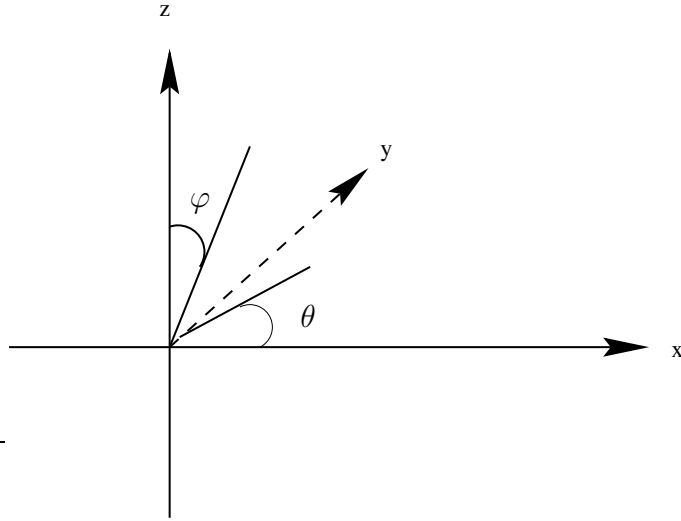


Figure 2.2: spherical coordinates

are

$$\begin{aligned}\lambda_1 &= u'n_1 + v'n_2 + w'n_3 + c', \\ \lambda_2 = \lambda_3 = \lambda_4 &= u'n_1 + v'n_2 + w'n_3, \\ \lambda_5 &= u'n_1 + v'n_2 + w'n_3 - c' .\end{aligned}$$

Where

$$\mathbf{n} = (n_1, n_2, n_3)^T = (\cos \theta \sin \varphi, \sin \theta \sin \varphi, \cos \varphi)^T \in \mathbb{R}^3$$

with $\theta \in [0, 2\pi]$ and $\varphi \in [0, \pi]$, see, Figure 2.2 and the corresponding linearly independent eigenvectors are

$$\mathbf{r}_1 := \begin{pmatrix} -\rho'/c' \\ n_1 \\ n_2 \\ n_3 \\ -\rho'c' \end{pmatrix}, \mathbf{r}_2 := \begin{pmatrix} 0 \\ n_2 \\ -n_1 \\ 0 \\ 0 \end{pmatrix}, \mathbf{r}_3 := \begin{pmatrix} 1 \\ 0 \\ 0 \\ 0 \\ 0 \end{pmatrix},$$

$$\mathbf{r}_4 := \begin{pmatrix} 0 \\ n_3 \\ 0 \\ -n_1 \\ 0 \end{pmatrix}, \mathbf{r}_5 := \begin{pmatrix} \rho'/c' \\ n_1 \\ n_2 \\ n_3 \\ \rho'c' \end{pmatrix}$$

Let $\mathcal{R}(\mathbf{U}')$ be the matrix of eigenvectors.
The inverse of $\mathcal{R}(\mathbf{U}')$ is

$$\mathcal{R}^{-1} := \begin{pmatrix} 0 & \frac{n_1}{2} & \frac{n_2}{2} & \frac{n_3}{2} & -\frac{1}{2\rho'c'} \\ 0 & n_2 & -\frac{n_3^2+n_1^2}{n_1} & \frac{n_2n_3}{n_1} & 0 \\ 1 & 0 & 0 & 0 & -\frac{1}{c'} \\ 0 & n_3 & \frac{n_2n_3}{n_1} & -\frac{n_2^2+n_1^2}{n_1} & 0 \\ 0 & \frac{n_1}{2} & \frac{n_2}{2} & \frac{n_3}{2} & \frac{1}{2\rho'c'} \end{pmatrix}$$

Multiplying system (2.2.8) by \mathcal{R}^{-1} from the left yields the characteristic system

$$\mathcal{W}_t + \mathcal{B}_1(\mathbf{U}')\mathcal{W}_x + \mathcal{B}_2(\mathbf{U}')\mathcal{W}_y + \mathcal{B}_3(\mathbf{U}')\mathcal{W}_z = 0 \quad (2.2.10)$$

where

$$\mathcal{B}_1 := \begin{pmatrix} u' - c'n_1 & -\frac{c'n_2}{2} & 0 & -\frac{c'n_3}{2} & 0 \\ -c'n_2 & u' & 0 & 0 & c'n_2 \\ 0 & 0 & u' & 0 & 0 \\ -c'n_3 & 0 & 0 & u' & c'n_3 \\ 0 & \frac{c'n_2}{2} & 0 & \frac{c'n_3}{2} & u' + c'n_1 \end{pmatrix},$$

$$\mathcal{B}_2 := \begin{pmatrix} v' - c'n_2 & \frac{c'n_1}{2} & 0 & 0 & 0 \\ c'(\frac{n_1^2+n_3^2}{n_1}) & v' & 0 & 0 & -c'(\frac{n_1^2+n_3^2}{n_1}) \\ 0 & 0 & v' & 0 & 0 \\ -\frac{c'n_2n_3}{n_1} & 0 & 0 & v' & \frac{c'n_2n_3}{n_1} \\ 0 & -\frac{c'n_1}{2} & 0 & 0 & v' + c'n_2 \end{pmatrix},$$

and

$$\mathcal{B}_3 := \begin{pmatrix} w' - c'n_3 & 0 & 0 & \frac{c'n_1}{2} & 0 \\ -\frac{c'n_2n_3}{n_1} & w' & 0 & 0 & \frac{c'n_2n_3}{n_1} \\ 0 & 0 & w' & 0 & 0 \\ c'(\frac{n_1^2+n_2^2}{n_1}) & 0 & 0 & w' & -c'(\frac{n_1^2+n_2^2}{n_1}) \\ 0 & 0 & 0 & -\frac{c'n_1}{2} & w' + c'n_3 \end{pmatrix}.$$

And the characteristic variables \mathcal{W} are

$$\mathbf{W} := \begin{pmatrix} w_1 \\ w_2 \\ w_3 \\ w_4 \\ w_5 \end{pmatrix} := \mathcal{R}^{-1}(\mathbf{U}')\mathbf{U} := \begin{pmatrix} \frac{1}{2}(n_1u + n_2v + n_3w - \frac{p}{\rho'c'}) \\ n_2u - \frac{n_1^2+n_3^2}{n_1}v + \frac{n_2n_3}{n_1}w \\ \rho - \frac{p}{c'^2} \\ n_3u + \frac{n_2n_3}{n_1}v - \frac{n_1^2+n_2^2}{n_1}w \\ \frac{1}{2}(n_1u + n_2v + n_3w + \frac{p}{\rho'c'}) \end{pmatrix}.$$

The quasi diagonalized system of the linearized Euler equations will be

$$\begin{aligned}
& \mathcal{W}_t + \begin{pmatrix} u' - c'n_1 & 0 & 0 & 0 & 0 \\ 0 & u' & 0 & 0 & 0 \\ 0 & 0 & u' & 0 & 0 \\ 0 & 0 & 0 & u' & 0 \\ 0 & 0 & 0 & 0 & u' + c'n_1 \end{pmatrix} \mathcal{W}_x \\
& + \begin{pmatrix} v' - c'n_2 & 0 & 0 & 0 & 0 \\ 0 & v' & 0 & 0 & 0 \\ 0 & 0 & v' & 0 & 0 \\ 0 & 0 & 0 & v' & 0 \\ 0 & 0 & 0 & 0 & v' + c'n_2 \end{pmatrix} \mathcal{W}_y \\
& + \begin{pmatrix} w' - c'n_3 & 0 & 0 & 0 & 0 \\ 0 & w' & 0 & 0 & 0 \\ 0 & 0 & w' & 0 & 0 \\ 0 & 0 & 0 & w' & 0 \\ 0 & 0 & 0 & 0 & w' + c'n_3 \end{pmatrix} \mathcal{W}_z = S \quad (2.2.11)
\end{aligned}$$

with

$$\mathbf{S} := \begin{pmatrix} s_1 \\ s_2 \\ s_3 \\ s_4 \\ s_5 \end{pmatrix} := \begin{pmatrix} \frac{c'}{2}(n_2 w_{2x} + n_3 w_{4x} - n_1 w_{2y} - n_1 w_{4z}) \\ c'n_2(w_{1x} - w_{5x}) - \frac{n_1^2 + n_3^2}{n_1}(w_{1y} - w_{5y}) + \left(\frac{n_2 n_3}{n_1}\right)(w_{1z} - w_{5z}) \\ 0 \\ c'(n_3(w_{1x} - w_{5x}) + \frac{n_2 n_3}{n_1}(w_{1y} - w_{5y}) - \frac{n_1^2 + n_2^2}{n_1}(w_{1z} - w_{5z})) \\ -\frac{c'}{2}(n_2 w_{2x} + n_3 w_{4x} - n_1 w_{2y} - n_1 w_{4z}) \end{pmatrix}.$$

Now we will work with the concept of bicharacteristics. The set of bicharacteristics \mathbf{x}_i corresponding to the i th equation of the system (2.2) is defined as

$$\frac{d\mathbf{x}_i}{d\tilde{t}} = \mathbf{b}_{ii}(\mathbf{n}) = (\mathbf{b}_{ii}^1, \mathbf{b}_{ii}^2, \dots, \mathbf{b}_{ii}^d)^T, i = 1, \dots, p.$$

Here b_{ii}^k are the diagonal entries of the matrix \mathcal{B}_k , $k = 1, \dots, d$, $i = 1, \dots, p$. Thus

$$\mathbf{x} = \mathbf{b}_{ii}\tilde{t} + c.$$

Applying the initial condition $\mathbf{x}_i(\mathbf{n}, t + \Delta t) = \mathbf{x}$, we get

$$\mathbf{x} = \mathbf{b}_{ii}(t + \Delta t) + c,$$

which implies that

$$c = \mathbf{x} - \mathbf{b}_{ii}(t + \Delta t).$$

Therefore

$$\mathbf{x}_i(\mathbf{n}, t) = \mathbf{x} - \mathbf{b}_{ii}(t + \Delta t - \tilde{t}).$$

Hence

$$Q_i(\mathbf{x}_i(\mathbf{n}, t), t) = (\mathbf{x} - b_{ii}\Delta t, t).$$

Now substituting for b_{ii} , $i = 1, 2, 3, 4$ from \mathcal{B}_k , $k = 1, 2, 3$ we get

$$Q_1 = (x - (u' - c'n_1)\Delta t, y - (v' - c'n_2)\Delta t, z - (w' - c'n_3)\Delta t, t)$$

$$Q_2 = Q_3 = Q_4 = (x - u'\Delta t, y - v'\Delta t, z - u'\Delta t, t)$$

$$Q_5 = (x - (u' + c'n_1)\Delta t, y - (v' + c'n_2)\Delta t, z - (w' + c'n_3)\Delta t, t)$$

We integrate the i th equation of the system(2.2.11) from the apex $P = (x, y, z, t + \Delta t)$ down to the footpoints $Q_i(\mathbf{n})$. Where the foot points of the corresponding bicharateristics are given above.

integration of system (2.2.11) along the bicharacteristics gives the relations for the characteristics variables, which after the multiplication from the left by the matrix \mathbf{R} yields the exact integral equations.

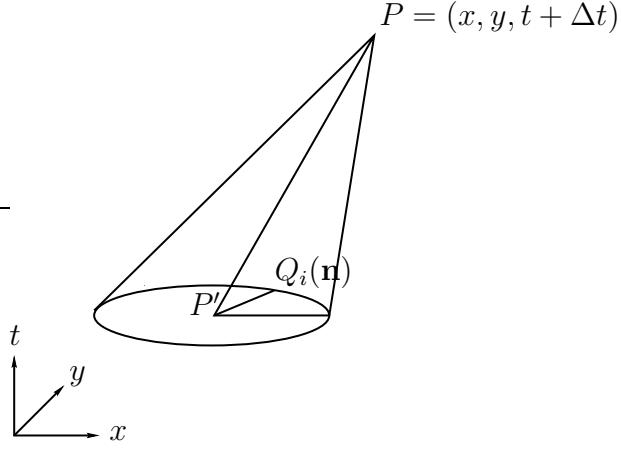


Figure 2.3: Bicharacteristics along the Mach cone through P and $Q_i(\mathbf{n})$, $d = 2$.

$$\begin{aligned}
 \mathbf{U}(P) := & \frac{1}{4\pi} \int_0^{2\pi} \int_0^\pi \left(\begin{array}{c} -\frac{\rho'}{c'} w_1 + w_3 + \frac{\rho'}{c'} w_5 \\ n_1 w_1 + n_2 w_2 + n_3 w_4 + n_1 w_5 \\ n_2 w_1 - n_1 w_2 + n_2 w_5 \\ n_3 w_1 - n_1 w_4 + n_3 w_5 \\ -\rho' c' w_1 + \rho' c' w_5 \end{array} \right) \\
 & + \left(\begin{array}{c} -\frac{\rho'}{c'} s_1' + \frac{\rho'}{c'} s_5' \\ n_1 s_1' + n_2 s_2' + n_3 s_4' + n_1 s_5' \\ n_2 s_1' - n_1 s_2' + n_2 s_5' \\ n_3 s_1' - n_1 s_4' + n_3 s_5' \\ -\rho' c' s_1' + \rho' c' s_5' \end{array} \right) \sin \varphi d\varphi d\theta \quad (2.2.12)
 \end{aligned}$$

where $S_i' = \int_t^{t+\Delta t} S_i(\mathbf{x}_i(\tilde{t}, \theta, \varphi), \tilde{t}, \theta, \varphi) d\tilde{t}$.

In the following two lemmas we give some invariance properties for terms in spherical coordinates.

Let f be a continuous function, and consider the unit sphere O centred at the origin. Let $x = \cos \theta \sin \varphi$, $y = \sin \theta \sin \varphi$, $z = \cos \varphi$. Then the integral of f over O satisfies the following property:

Lemma 2.2.1

$$\int_0^{2\pi} \int_{\pi}^{2\pi} f(x, y, z) \sin \varphi d\varphi d\theta = - \int_0^{2\pi} \int_0^{\pi} f(x, y, z) \sin \varphi d\varphi d\theta.$$

Proof: The proof follows directly from the fact that the mappings

$$\psi_1 : [0, 2\pi] \times [\pi, 2\pi] \rightarrow O \subset \mathbb{R}^3, (\theta, \varphi) \mapsto (\cos \theta \sin \varphi, \sin \theta \sin \varphi, \cos \varphi),$$

$$\psi_2 : [0, 2\pi] \times [\pi, 2\pi] \rightarrow O \subset \mathbb{R}^3, (\theta, \varphi) \mapsto (-\cos \theta \sin \varphi, -\sin \theta \sin \varphi, -\cos \varphi)$$

are two parametrizations of the same unit sphere O . □

Corollary 2.2.1 *Let $a \in \mathbb{R}$ be a constant. Then*

1. $\int_0^{2\pi} \int_{\pi}^{2\pi} (a+x)f(x, y, z) \sin \varphi d\varphi d\theta = - \int_0^{2\pi} \int_0^{\pi} (a+x)f(x, y, z) \sin \varphi d\varphi d\theta.$
2. $\int_0^{2\pi} \int_{\pi}^{2\pi} (a+y)f(x, y, z) \sin \varphi d\varphi d\theta = - \int_0^{2\pi} \int_0^{\pi} (a+y)f(x, y, z) \sin \varphi d\varphi d\theta.$
3. $\int_0^{2\pi} \int_{\pi}^{2\pi} (a+z)f(x, y, z) \sin \varphi d\varphi d\theta = - \int_0^{2\pi} \int_0^{\pi} (a+z)f(x, y, z) \sin \varphi d\varphi d\theta.$

Proof: These properties follow from Lemma 2.2.1 by taking $g = (a + \xi)f(x, y, z)$, where $\xi \in \{x, y, z\}$. □

Lemma 2.2.2 *Consider the characteristic variables w_1 and w_5 and the points Q_1 and Q_5 . Then*

1. $\sin(\pi + \varphi)w_5(Q_5(\theta, \pi + \varphi), \theta, \pi + \varphi) = \sin \varphi w_1(Q_1(\theta, \varphi), \theta, \varphi).$

2. $\sin(\pi + \varphi) \sin(\pi + \varphi) w_5(Q_5(\theta, \pi + \varphi), \theta, \pi + \varphi)$
 $= -\sin \varphi \sin \varphi w_1(Q_1(\theta, \varphi), \theta, \varphi).$
3. $\cos(\pi + \varphi) \sin(\pi + \varphi) w_5(Q_5(\theta, \pi + \varphi), \theta, \pi + \varphi)$
 $= -\cos \varphi \sin \varphi w_1(Q_1(\theta, \varphi), \theta, \varphi).$

Proof: Using the symmetry between the points Q_1 and Q_5 we obtain

$$\begin{aligned}
& w_5(Q_5(\theta, \pi + \varphi), \theta, \pi + \varphi) \\
&= \frac{1}{2} \left[\frac{P}{\rho' c'}(Q_5(\theta, \pi + \varphi)) + \cos \theta \sin(\pi + \varphi) u(Q_5(\theta, \pi + \varphi)) \right. \\
&\quad \left. + \sin \theta \sin(\pi + \varphi) v(Q_5(\theta, \pi + \varphi)) + \cos(\pi + \varphi) w(Q_5(\theta, \pi + \varphi)) \right] \\
&= \frac{1}{2} \left[\frac{P}{\rho' c'}(Q_1(\theta, \varphi)) - \cos \theta \sin \varphi u(Q_1(\theta, \varphi)) - \sin \theta \sin \varphi v(Q_1(\theta, \varphi)) \right. \\
&\quad \left. - \cos \varphi w(Q_1(\theta, \varphi)) \right] = -w_1(Q_1(\theta, \varphi), \theta, \varphi).
\end{aligned} \tag{2.2.13}$$

Now the three properties follow directly from equation (2.2.13).

□

Then using these results, the exact integral equations will be :

$$\begin{aligned}
\rho(P) &= \rho(P') - \frac{p(P')}{c'^2} \\
&\quad + \frac{1}{4\pi} \int_0^{2\pi} \int_0^\pi \left[\frac{p(Q)}{c'^2} - \frac{\rho'}{c'} u(Q) n_1 - \frac{\rho'}{c'} v(Q) n_2 - \frac{\rho'}{c'} w(Q) n_3 \right] \sin \varphi \, d\varphi \, d\theta + \tilde{S}_1
\end{aligned} \tag{2.2.14}$$

$$u(P) = \frac{2}{3}u(P') + \tag{2.2.15}$$

$$\frac{1}{4\pi} \int_0^{2\pi} \int_0^\pi n_1 \left[-\frac{p(Q)}{\rho'c'} + u(Q)n_1 + v(Q)n_2 + w(Q)n_3 \right] \sin \varphi \, d\varphi \, d\theta + \tilde{S}_2$$

$$v(P) = \frac{2}{3}v(P') \tag{2.2.16}$$

$$+ \frac{1}{4\pi} \int_0^{2\pi} \int_0^\pi n_2 \left[-\frac{p(Q)}{\rho'c'} + u(Q)n_1 + v(Q)n_2 + w(Q)n_3 \right] \sin \varphi \, d\varphi \, d\theta + \tilde{S}_3$$

$$w(P) = \frac{2}{3}w(P') \tag{2.2.17}$$

$$+ \frac{1}{4\pi} \int_0^{2\pi} \int_0^\pi n_3 \left[-\frac{p(Q)}{\rho'c'} + n_1u(Q) + n_2v(Q) + n_3w(Q) \right] \sin \varphi \, d\varphi \, d\theta + S_4.$$

$$p(P) = \frac{1}{4\pi} \int_0^{2\pi} \int_0^\pi \left[p(Q) - \rho'c'u(Q)n_1 - \rho'c'v(Q)n_2 - \rho'c'w(Q)n_3 \right] \sin \varphi \, d\varphi \, d\theta + \tilde{S}_5 \tag{2.2.18}$$

where

$$\tilde{S}_1 = \frac{1}{4\pi} \int_0^{2\pi} \int_0^\pi \left[\frac{-\rho'}{c'}S_1' + \frac{\rho'}{c'}S_5' \right] \sin \varphi \, d\varphi \, d\theta, \tag{2.2.19}$$

$$\tilde{S}_2 = \frac{1}{4\pi} \int_0^{2\pi} \int_0^\pi \left[n_1S_1' + n_2S_2' + n_3S_4' + n_1S_5' \right] \sin \varphi \, d\varphi \, d\theta, \tag{2.2.20}$$

$$\tilde{S}_3 = \frac{1}{4\pi} \int_0^{2\pi} \int_0^\pi \left[n_2S_1' - n_1S_2' + n_2S_5' \right] \sin \varphi \, d\varphi \, d\theta, \tag{2.2.21}$$

$$\tilde{S}_4 = \frac{1}{4\pi} \int_0^{2\pi} \int_0^\pi \left[n_3S_1' - n_1S_4' + n_1S_5' \right] \sin \varphi \, d\varphi \, d\theta, \tag{2.2.22}$$

$$\tilde{S}_5 = \frac{1}{4\pi} \int_0^{2\pi} \int_0^\pi \left[-\rho'c'S_1' + \rho'c'S_5' \right] \sin \varphi \, d\varphi \, d\theta. \tag{2.2.23}$$

We will explain the derivation of $\rho(P)$, and $u(P)$, and the others can be similarly handled.

From equation (2.2.12) we see that

$$\rho(P) = \frac{1}{4\pi} \int_0^{2\pi} \int_0^\pi \left[\frac{-\rho'}{c'} w_1 + w_3 + \frac{\rho'}{c'} w_5 \right] \sin \varphi \, d\varphi \, d\theta + \tilde{S}_1. \quad (2.2.24)$$

where \tilde{S}_1 is defined above. Now since w_3 is independent of θ, φ we can find that

$$\frac{1}{4\pi} \int_0^{2\pi} \int_0^\pi w_3(Q_3) \sin \varphi \, d\varphi \, d\theta = \rho(p') - \frac{p(p')}{c'^2}.$$

Using the symmetry between the points Q_1 and Q_5 and lemma(2.2.2) we see that

$$\begin{aligned} & \int_0^{2\pi} \int_0^\pi -w_1(Q_1(\theta, \varphi), \theta, \varphi) \sin \varphi \, d\varphi \, d\theta \\ = & \int_0^{2\pi} \int_0^\pi -w_5(Q_5(\theta, \varphi + \pi), \theta, \varphi + \pi) \sin(\varphi + \pi) \, d\varphi \, d\theta \\ = & \int_0^{2\pi} \int_\pi^{2\pi} -w_5(Q_5(\theta, \varphi), \theta, \varphi) \sin \varphi \, d\varphi \, d\theta \\ = & \int_0^{2\pi} \int_0^\pi w_5(Q_5(\theta, \varphi), \theta, \varphi) \sin \varphi \, d\varphi \, d\theta. \end{aligned}$$

and hence

$$\begin{aligned} & \int_0^{2\pi} \int_0^\pi w_5(Q_5(\theta, \varphi), \theta, \varphi) \sin \varphi \, d\varphi \, d\theta \\ = & \int_0^{2\pi} \int_0^\pi -w_1(Q_1(\theta, \varphi), \theta, \varphi) \sin \varphi \, d\varphi \, d\theta, \end{aligned}$$

substituting in equation (2.2.24), it comes that

$$\rho(P) = \rho(P') - \frac{p(P')}{c'^2} + \frac{1}{4\pi} \int_0^{2\pi} \int_0^\pi \left[-2 \frac{-\rho'}{c'} w_1 \right] \sin \varphi d\varphi d\theta + \tilde{S}_1. \quad (2.2.25)$$

Now substituting for w_1 in (2.2.25), we find that

$$\begin{aligned} \rho(P) = \rho(P') - \frac{p(P')}{c'^2} + \frac{1}{4\pi} \int_0^{2\pi} \int_0^\pi \left[\frac{p(Q)}{c'^2} - \frac{\rho'}{c'} n_1 u(Q) - \frac{\rho'}{c'} n_2 v(Q) \right. \\ \left. - \frac{\rho'}{c'} n_3 w(Q) \right] \sin \varphi d\varphi d\theta + \tilde{S}_1. \end{aligned}$$

Where $Q := Q_1$.

To derive $u(P)$ we recall from equation (2.2.12) that

$$u(P) = \frac{1}{4\pi} \int_0^{2\pi} \int_0^\pi [n_1 w_1 + n_2 w_2 + n_3 w_4 + n_1 w_5] \sin \varphi d\varphi d\theta + \tilde{S}_2. \quad (2.2.26)$$

We see that

$$\begin{aligned} & \frac{1}{4\pi} \int_0^{2\pi} \int_0^\pi [n_2 w_2 + n_3 w_3] \sin \varphi d\varphi d\theta \\ = & \frac{1}{4\pi} \int_0^{2\pi} \int_0^\pi \left[n_2^2 u - n_2 \left(\frac{n_1^2 + n_3^2}{n_1} \right) v + \frac{n_2^2 n_3}{n_1} w_{Q_2} \right. \\ & \left. + n_3^2 u_{Q_4} + \frac{n_2 n_3^2}{n_1} v_{Q_4} - n_3 \frac{n_1^2 + n_2^2}{n_1} w_{Q_4} \right] \sin \varphi d\varphi d\theta \\ = & \frac{1}{2\pi} \int_0^\pi \left[(n_2^2 + n_3^2) u_{Q_2} - n_2 n_1 v_{Q_2} - n_1 n_3 w_{Q_2} \right] \sin \varphi d\varphi d\theta \end{aligned}$$

$$\begin{aligned}
&= \frac{1}{4\pi} \int_0^{2\pi} \int_0^\pi [(n_2^2 + n_3^2)u_{Q_2} - n_1n_2v_{Q_2} - n_1n_3w_{Q_2}] \sin \varphi d\varphi d\theta \\
&= \frac{2}{3}u_{Q_2} \\
&= \frac{2}{3}u(P').
\end{aligned}$$

For

$$\frac{1}{4\pi} \int_0^{2\pi} \int_0^\pi (n_1w_1 + n_1w_5) \sin \varphi d\varphi d\theta$$

we see that, using (2) of lemma(2.2.2) and (2) of Corollary (2.2.1) we obtain

$$\begin{aligned}
&\int_0^{2\pi} \int_0^\pi (\cos \theta \sin \varphi \sin \varphi w_1(Q_1(\theta, \varphi), \theta, \varphi) d\varphi d\theta \\
&= \int_0^{2\pi} \int_0^\pi -(\cos \theta \sin(\pi + \varphi) \sin(\pi + \varphi) w_5(Q_5(\theta, \pi + \varphi), \theta, \pi + \varphi) d\varphi d\theta \\
&= \int_0^{2\pi} \int_\pi^{2\pi} -(\cos \theta \sin \varphi w_5(Q_5(\theta, \varphi), \theta, \varphi) \sin \varphi d\varphi d\theta, \\
&= \int_0^{2\pi} \int_0^\pi (\cos \theta \sin \varphi w_5(Q_5(\theta, \varphi), \theta, \varphi) \sin \varphi d\varphi d\theta.
\end{aligned}$$

Therefore

$$\begin{aligned}
&\int_0^{2\pi} \int_0^\pi (\cos \theta \sin \varphi w_5(Q_5(\theta, \varphi), \theta, \varphi) \sin \varphi d\varphi d\theta \\
&= \int_0^{2\pi} \int_0^\pi (\cos \theta \sin \varphi w_1(Q_1(\theta, \varphi), \theta, \varphi) \sin \varphi d\varphi d\theta.
\end{aligned}$$

so after substituting in equation (2.2.26) we end up with

$$u(P) = \frac{2}{3}u(P') + \frac{1}{4\pi} \int_0^{2\pi} \int_0^\pi n_1 \left[-\frac{p(Q)}{\rho'c'} + n_1 u(Q) + n_2 v(Q) + n_3 w(Q) \right] \sin \varphi \, d\varphi \, d\theta + \tilde{S}_2. \quad (2.2.27)$$

Our attention now is to simplify the source terms $\tilde{S}_1, \tilde{S}_2, \tilde{S}_3, \tilde{S}_4, \tilde{S}_5$ which will be used in the derivation of the approximate evolution operators.

From(2.2.12) we see that

$$\begin{aligned} S_1 &= \frac{c'}{2} \left[n_2 w_{2x} + n_3 w_{4x} + n_1 w_{2y} - n_1 w_{4z} \right] \\ &= \frac{c'}{2} \left[n_2^2 u_x - n_2 \frac{n_1^2 + n_3^2}{n_1} v_x + \frac{n_2^2 n_3}{n_1} w_x + n_3^2 u_x \right. \\ &\quad \left. + \frac{n_2 n_3^2}{n_1} v_x - n_3 \frac{n_1^2 + n_2^2}{n_1} w_x - n_1 n_2 u_y + (n_1^2 + n_3^2) v_y \right. \\ &\quad \left. - n_2 n_3 w_y - n_1 n_3 u_z - n_2 n_3 v_z + (n_1^2 + n_2^2) w_z \right] \end{aligned} \quad (2.2.28)$$

$$\begin{aligned} &= \frac{c'}{2} \left[(n_2^2 + n_3^2) u_x - n_1 n_2 v_x - n_1 n_3 w_x - n_1 n_2 u_y + (n_1^2 + n_3^2) v_y - n_2 n_3 w_y \right. \\ &\quad \left. - n_1 n_3 u_z - n_2 n_3 v_z + (n_1^2 + n_2^2) w_z \right]. \end{aligned} \quad (2.2.29)$$

In the same procedure we found that

$$S_2 = -\frac{1}{\rho'} \left[n_2 p_x + \frac{n_1^2 + n_3^2}{n_1} p_y - \frac{n_2 n_3}{n_1} p_z \right] \quad (2.2.30)$$

$$S_4 = -\frac{1}{\rho'} \left[n_3 p_x + \frac{n_2 n_3}{n_1} p_y - \frac{n_1^2 + n_2^2}{n_1} p_z \right] \quad (2.2.31)$$

$$S_5 = -\frac{c'}{2} \left[(n_2^2 + n_3^2)u_x - n_1n_2v_x - n_1n_3w_x + n_1n_2u_y - (n_1^2 + n_3^2)v_y \right. \\ \left. + n_2n_3w_y + n_1n_3u_z + n_2n_3v_z - (n_1^2 + n_2^2)w_z \right]. \quad (2.2.32)$$

Now let

$$S = c' \left[(n_2^2 + n_3^2)u_x - n_1n_2(v_x + u_y) - n_1n_3(u_z + w_x) + (n_1^2 + n_3^2)v_y - n_2n_3(w_y + v_z) + (n_1^2 + n_2^2)w_z \right]. \quad (2.2.33)$$

Now simplifying \tilde{S}_1 we have

$$\begin{aligned} \tilde{S}_1 &= \frac{1}{4\pi} \int_0^{2\pi} \int_0^\pi \int_0^{\Delta t} \left[\frac{-\rho'}{c'} S_1 + \frac{-\rho'}{c'} S_5 \right] \sin \varphi \, d\varphi \, d\theta \\ &= \frac{1}{4\pi} \int_0^{2\pi} \int_0^\pi \int_0^{\Delta t} \left[\frac{-\rho'}{c'} (S_1 + S_5) \right] \sin \varphi \, d\varphi \, d\theta \\ &= \frac{1}{4\pi} \int_0^{2\pi} \int_0^\pi \int_0^{\Delta t} \left[\frac{-\rho'}{c'} S(\mathbf{x} - (u' - c'\mathbf{w}(\theta, \varphi))\tau, t + \Delta t - \tau, \theta, \varphi) \right] \sin \varphi \, d\tau \, d\varphi \, d\theta. \end{aligned} \quad (2.2.34)$$

Following the same procedure we can simplify $\tilde{S}_2, \tilde{S}_3, \tilde{S}_4, \tilde{S}_5$, and we find that

$$\begin{aligned} \tilde{S}_2 &= \frac{1}{4\pi} \int_0^{2\pi} \int_0^\pi \int_0^{\Delta t} \left[n_1 S(\mathbf{x} - (u' - c'\mathbf{w}(\theta, \varphi))\tau, t + \Delta t - \tau, \theta, \varphi) \right] \sin \varphi \, d\tau \, d\varphi \, d\theta \\ &\quad - \frac{1}{\rho' 4\pi} \int_0^{2\pi} \int_0^\pi \int_0^{\Delta t} [p_x(x, t)(n_2^2 + n_3^2) - p_y(x, t)n_1n_2 - p_zn_1n_3] \sin \varphi \, d\tau \, d\varphi \, d\theta \end{aligned} \quad (2.2.35)$$

$$\begin{aligned} \tilde{S}_3 &= \frac{1}{4\pi} \int_0^{2\pi} \int_0^\pi \int_0^{\Delta t} \left[n_2 S(\mathbf{x} - (u' - c'\mathbf{w}(\theta, \varphi))\tau, t + \Delta t - \tau, \theta, \varphi) \right] \sin \varphi \, d\tau \, d\varphi \, d\theta \\ &\quad - \frac{1}{\rho' 4\pi} \int_0^{2\pi} \int_0^\pi \int_0^{\Delta t} [p_y(x, t)(n_1^2 + n_3^2) - p_z(x, t)n_2n_3 - p_xn_1n_2] \sin \varphi \, d\tau \, d\varphi \, d\theta \end{aligned} \quad (2.2.36)$$

$$\begin{aligned}
\tilde{S}_4 = & \frac{1}{4\pi} \int_0^{2\pi} \int_0^\pi \int_0^{\Delta t} \left[n_3 S(\mathbf{x} - (u' - c' \mathbf{w}(\theta, \varphi))\tau, t + \Delta t - \tau, \theta, \varphi) \right] \sin \varphi \, d\tau \, d\varphi \, d\theta \\
& - \frac{1}{\rho' 4\pi} \int_0^{2\pi} \int_0^\pi \int_0^{\Delta t} [p_z(x, t)(n_1^2 + n_2^2) - p_y(x, t)n_2 n_3 - p_x n_1 n_3] \sin \varphi \, d\tau \, d\varphi \, d\theta
\end{aligned} \tag{2.2.37}$$

$$\tilde{S}_5 = -\frac{\rho' c'}{4\pi} \int_0^{2\pi} \int_0^\pi \int_0^{\Delta t} \left[S(\mathbf{x} - (u' - c' \mathbf{w}(\theta, \varphi))\tau, t + \Delta t - \tau, \theta, \varphi) \right] \sin \varphi \, d\tau \, d\varphi \, d\theta \tag{2.2.38}$$

hence we have the following integral equations

$$\begin{aligned}
\rho(P) = & \rho(P') - \frac{p(P')}{c'^2} + \tag{2.2.39} \\
& \frac{1}{4\pi} \int_0^{2\pi} \int_0^\pi \left[\frac{p(Q)}{c'^2} - \frac{\rho'}{c'} n_1 u(Q) - \frac{\rho'}{c'} n_2 v(Q) - \frac{\rho'}{c'} n_3 w(Q) \right] \sin \varphi \, d\varphi \, d\theta + \tilde{S}_1
\end{aligned}$$

$$\begin{aligned}
u(P) = & \frac{2}{3} u(P') + \tag{2.2.40} \\
& \frac{1}{4\pi} \int_0^{2\pi} \int_0^\pi n_1 \left[-\frac{p(Q)}{\rho' c'} + n_1 u(Q) + n_2 v(Q) + n_3 w(Q) \right] \sin \varphi \, d\varphi \, d\theta + \tilde{S}_2
\end{aligned}$$

$$\begin{aligned}
v(P) = & \frac{2}{3} v(P') + \tag{2.2.41} \\
& \frac{1}{4\pi} \int_0^{2\pi} \int_0^\pi n_2 \left[-\frac{p(Q)}{\rho' c'} + n_1 u(Q) + n_2 v(Q) + n_3 w(Q) \right] \sin \varphi \, d\varphi \, d\theta + \tilde{S}_3
\end{aligned}$$

$$\begin{aligned}
w(P) = & \frac{2}{3} w(P') + \tag{2.2.42} \\
& \frac{1}{4\pi} \int_0^{2\pi} \int_0^\pi n_3 \left[-\frac{p(Q)}{\rho' c'} + n_1 u(Q) + n_2 v(Q) + n_3 w(Q) \right] \sin \varphi \, d\varphi \, d\theta + \tilde{S}_4
\end{aligned}$$

$$\begin{aligned}
p(P) = & \frac{1}{4\pi} \int_0^{2\pi} \int_0^\pi \left[\frac{p(Q)}{c'^2} - \frac{\rho'}{c'} n_1 u(Q) - \frac{\rho'}{c'} n_2 v(Q) - \frac{\rho'}{c'} n_3 w(Q) \right] \sin \varphi \, d\varphi \, d\theta + \tilde{S}_5 \tag{2.2.43}
\end{aligned}$$

where $\tilde{S}_1, \dots, \tilde{S}_5$ is given in equations (2.2.34-2.2.38).

Chapter 3

Evolution Galerkin Methods

3.1 Definition of Evolution Galerkin Schemes

Consider $d = 3$. and Let $h > 0$ be the mesh size parameter. We construct a mesh for \mathbb{R}^3 , which consists of the cubic mesh cells

$$\begin{aligned}\Omega_{klm} &= \left[\left(k - \frac{1}{2}\right)h, \left(k + \frac{1}{2}\right)h \right] \times \left[\left(l - \frac{1}{2}\right)h, \left(l + \frac{1}{2}\right)h \right] \times \left[\left(m - \frac{1}{2}\right)h, \left(m + \frac{1}{2}\right)h \right] \\ &= \left[x_k - \frac{h}{2}, x_k + \frac{h}{2} \right] \times \left[y_l - \frac{h}{2}, y_l + \frac{h}{2} \right] \times \left[z_m - \frac{h}{2}, z_m + \frac{h}{2} \right],\end{aligned}$$

where $k, l, m \in \mathbb{Z}$. Let us denote by $H^\kappa(\mathbb{R}^3)$ the Sobolev space of distributions with derivatives up to order κ in L^2 space, where $\kappa \in \mathbb{N}$. Consider the general hyperbolic system given by the equation (2.1.1). Let us denote by $E(s) : (H^\kappa(\mathbb{R}^3))^p \rightarrow (H^\kappa(\mathbb{R}^3))^p$ the exact evolution operator for the system (2.1.1), i.e.

$$\mathbf{u}(\cdot, t + s) = E(s)\mathbf{u}(\cdot, t). \quad (3.1.1)$$

We suppose that S_h^q is a finite element space consisting of piecewise polynomials of order $q \geq 0$ with respect to the cubic mesh. Assume a constant time step, i.e. $t_n = n\Delta t$. Let \mathbf{U}^n be an approximation in the space S_h^q to the exact solution $\mathbf{u}(\cdot, t_n)$ at time $t_n \geq 0$. We consider $E_\tau : (L_{loc}^1(\mathbb{R}^3)) \rightarrow (H^\kappa(\mathbb{R}^3))^p$ to be

a suitable approximate evolution operator for $E(\tau)$. In practice we will use restrictions of E_τ to the subspace S_h^q for $q \geq 0$. Then we can define the general class of evolution Galerkin methods.

Definition 3.1.2 *Starting from some initial data $\mathbf{u}^0 \in S_h^q$ at time $t = 0$, an evolution Galerkin method (EG-method) is recursively defined by means of*

$$\mathbf{U}^{n+1} = P_h E_\tau \mathbf{U}^n, \quad (3.1.2)$$

where P_h is the L^2 -projection given by the integral averages in the following way

$$P_h \mathbf{U}^n|_{\Omega_{klm}} = \frac{1}{|\Omega_{klm}|} \int_{\Omega_{klm}} \mathbf{U}(x, y, z, t_n) dx dy.$$

We denote by $R_h : S_h^q \rightarrow S_h^r$ a recovery operator, $r > q \geq 0$ and consider our approximate evolution operator E_τ on S_h^r . Taking piecewise constants, the resulting schemes will only be of first order, even when E_τ is approximated to a higher order. Higher order accuracy can be obtained either by taking $q > 0$, or by inserting a recovery stage R_h before the evolution step in equation (3.1.2) to give

$$\mathbf{U}^{n+1} = P_h E_\tau R_h \mathbf{U}^n. \quad (3.1.3)$$

This approach involves the computation of multiple integrals and becomes quite complex for higher order recoveries. To avoid this we will consider evolution Galerkin schemes based on the finite volume formulation instead.

Definition 3.1.5 *Starting from some initial data $\mathbf{u}^0 \in S_h^q$, the finite volume evolution Galerkin method (FVEG) is recursively*

defined by means of

$$\mathbf{U}^{n+1} = \mathbf{U}^n - \frac{1}{h} \int_0^{\Delta t} \sum_{j=1}^3 \delta_{x_j} \mathbf{f}_j(\tilde{\mathbf{U}}^{n+\frac{\tau}{\Delta t}}) d\tau, \quad (3.1.6)$$

where $\delta_{x_j} \mathbf{f}_j(\tilde{\mathbf{U}}^{n+\frac{\tau}{\Delta t}})$ represents an approximation to the face flux difference and δ_x is defined by $\delta_x = v(x + \frac{h}{2}) - v(x - \frac{h}{2})$. The cell boundary value $\tilde{\mathbf{U}}^{n+\frac{\tau}{\Delta t}}$ is evolved using the approximate evolution operator E_τ to $t_n + \tau$ and averaged along the cell boundary, i.e.

$$\tilde{\mathbf{U}}^{n+\frac{\tau}{\Delta t}} = \sum_{k,l,m \in \mathbb{Z}} \left(\frac{1}{|\partial\Omega_{klm}|} \int_{\partial\Omega_{klm}} E_\tau R_h \mathbf{U}^n dS \right) \chi_{\partial\Omega_{klm}}, \quad (3.1.7)$$

where $\chi_{\partial\Omega_{klm}}$ is the characteristic function of $\partial\Omega_{klm}$.

In this formulation a first order approximation E_τ to the exact operator $E(\tau)$ yields an overall higher order update from \mathbf{U}^n to \mathbf{U}^{n+1} . To obtain this approximation in the discrete scheme it is only necessary to carry out a recovery stage at each level to generate a piecewise polynomial approximation $\tilde{\mathbf{U}}^n = R_h \mathbf{U}^n \in S_h^r$ from the piecewise constant $\mathbf{U}^n \in S_h^0$, to feed into the calculation of the fluxes. It is important to note that in the updating step (3.1.6) some numerical quadratures are used instead of the exact time integration. Similarly, to evaluate the intermediate value $\tilde{\mathbf{U}}^{n+\frac{\tau}{\Delta t}}$ in (3.1.7) either the four dimensional integrals along the cell-interface and around the Mach cone are evaluated exactly or by means of suitable numerical quadratures..

3.2 Approximate Evolution Operators

The key ingredient in our genuinely multidimensional schemes are the approximate evolution operators that are derived from the integral equations. The integral equation is obtained using integration along the bicharacteristics of the system. From these integral equations one can derive a number of approximate evolution operators.

In this section we will derive two approximate evolution operators the EG1 and EG3, but in our numerical experiment we consider a third one which we call N1. This approximate evolution operator(N1) is the simplest one since it depends on neglecting the source terms in the integral equations and consider the other part as an approximate evolution operator. We examine this approximate evolution operator in our numerical experiments which gives results which are in good agreement with the exact solution in the linearized form.

$$\rho(P) = \rho(P') - \frac{p(P')}{c'^2} \quad (3.2.8)$$

$$+ \frac{1}{4\pi} \int_0^{2\pi} \int_0^\pi \left[\frac{p(Q)}{c'^2} - \frac{\rho'}{c'} u(Q)n_1 - \frac{\rho'}{c'} v(Q)n_2 - \frac{\rho'}{c'} w(Q)n_3 \right] \sin \varphi d\varphi d\theta + \tilde{S}_1$$

$$u(P) = \frac{2}{3}u(P') + \quad (3.2.9)$$

$$\frac{1}{4\pi} \int_0^{2\pi} \int_0^\pi n_1 \left[-\frac{p(Q)}{\rho'c'} + u(Q)n_1 + v(Q)n_2 + w(Q)n_3 \right] \sin \varphi d\varphi d\theta + \tilde{S}_2$$

$$v(P) = \frac{2}{3}v(P') \quad (3.2.10)$$

$$+ \frac{1}{4\pi} \int_0^{2\pi} \int_0^\pi n_2 \left[-\frac{p(Q)}{\rho'c'} + u(Q)n_1 + v(Q)n_2 + w(Q)n_3 \right] \sin \varphi d\varphi d\theta + \tilde{S}_3$$

$$w(P) = \frac{2}{3}w(P') \quad (3.2.11)$$

$$+ \frac{1}{4\pi} \int_0^{2\pi} \int_0^\pi n_3 \left[-\frac{p(Q)}{\rho'c'} + n_1u(Q) + n_2v(Q) + n_3w(Q) \right] \sin \varphi d\varphi d\theta + \tilde{S}_4.$$

$$p(P) = \frac{1}{4\pi} \int_0^{2\pi} \int_0^\pi \left[p(Q) - \rho'c'u(Q)n_1 - \rho'c'v(Q)n_2 - \rho'c'w(Q)n_3 \right] \sin \varphi d\varphi d\theta + \tilde{S}_5 \quad (3.2.12)$$

Now the integrals of the source term can be approximated using the rectangle rule,

$$\int_0^{\Delta t} \mathbf{S}_j(t + \Delta t - \tau, \theta, \varphi) = \Delta t \mathbf{S}_j(t, \theta, \varphi) + O(\Delta t^2),$$

and hence we have these approximations

$$\begin{aligned} \tilde{S}_1 &= \frac{\Delta t}{4\pi} \int_0^{2\pi} \int_0^\pi \left[\frac{-\rho'}{c'} S(\mathbf{x} - (u' - c' \mathbf{w}(\theta, \varphi))\tau, t + \Delta t - \tau, \theta, \varphi) \right] \sin \varphi d\tau d\varphi d\theta + O(\Delta t^2) \\ \tilde{S}_2 &= \frac{\Delta t}{4\pi} \int_0^{2\pi} \int_0^\pi \left[n_1 S(\mathbf{x} - (u' - c' \mathbf{w}(\theta, \varphi))\tau, t + \Delta t - \tau, \theta, \varphi) \right] \sin \varphi d\tau d\varphi d\theta + \\ &\quad - \frac{1}{\rho'} \frac{1}{4\pi} \int_0^{2\pi} \int_0^\pi [p_x(x, t)(n_2^2 + n_3^2) - p_y(x, t)n_1n_2 - p_zn_1n_3] \sin \varphi : d\varphi d\theta + O(\Delta t^2) \\ \tilde{S}_3 &= \frac{\Delta t}{4\pi} \int_0^{2\pi} \int_0^\pi \left[n_2 S(\mathbf{x} - (u' - c' \mathbf{w}(\theta, \varphi))\tau, t + \Delta t - \tau, \theta, \varphi) \right] \sin \varphi d\tau d\varphi d\theta \\ &\quad - \frac{1}{\rho'} \frac{1}{4\pi} \int_0^{2\pi} \int_0^\pi [p_y(x, t)(n_1^2 + n_3^2) - p_z(x, t)n_2n_3 - p_xn_1n_2] \sin \varphi d\tau : d\varphi d\theta + O(\Delta t^2) \\ \tilde{S}_4 &= \frac{\Delta t}{4\pi} \int_0^{2\pi} \int_0^\pi \left[n_3 S(\mathbf{x} - (u' - c' \mathbf{w}(\theta, \varphi))\tau, t + \Delta t - \tau, \theta, \varphi) \right] \sin \varphi d\tau d\varphi d\theta \\ &\quad - \frac{\Delta t}{4\pi} \int_0^{2\pi} \int_0^\pi \int_0^{\Delta t} [p_z(x, t)(n_1^2 + n_2^2) - p_y(x, t)n_2n_3 - p_xn_1n_3] \sin \varphi d\varphi d\theta + O(\Delta t^2) \\ \tilde{S}_5 &= -\Delta t \frac{\rho' c'}{4\pi} \int_0^{2\pi} \int_0^\pi \int_0^{\Delta t} \left[\frac{-\rho'}{c'} S(\mathbf{x} - (u' - c' \mathbf{w}(\theta, \varphi))\tau, t + \Delta t - \tau, \theta, \varphi) \right] \sin \varphi d\tau d\varphi d\theta \\ &\quad + O(\Delta t^2) \end{aligned}$$

Lemma 3.2.1

$$\begin{aligned} &\frac{\Delta t}{4\pi} \int_0^{2\pi} \int_0^\pi \left[S(\mathbf{x} - (u' - c' \mathbf{w}(\theta, \varphi))\tau, t + \Delta t - \tau, \theta, \varphi) \right] \sin \varphi d\tau d\varphi d\theta \\ &= \frac{1}{4\pi} \int_0^{2\pi} \int_0^\pi [2n_1u_Q + 2n_2v_Q + 2n_3w_Q] \sin \varphi d\varphi d\theta \end{aligned}$$

where $Q = (\mathbf{x} - (u' - c' \mathbf{w}(\theta, \varphi))\tau, t + \Delta t - \tau, \theta, \varphi)$

Proof: see [19]. □

similarly we can find that

$$\begin{aligned} & \frac{\Delta t}{4\pi} \int_0^{2\pi} \int_0^\pi \left[n_1 S(\mathbf{x} - (u' - c' \mathbf{w}(\theta, \varphi))\tau, t + \Delta t - \tau, \theta, \varphi) \right] \sin \varphi d\varphi d\theta \\ &= \frac{1}{4\pi} \int_0^{2\pi} \int_0^\pi \left[(3n_1^2 - 1)u_Q + 3n_1 n_2 v_Q + 3n_1 n_3 w_Q \right] \sin \varphi d\varphi d\theta \end{aligned}$$

and

$$\begin{aligned} & \frac{\Delta t}{4\pi} \int_0^{2\pi} \int_0^\pi \left[n_2 S(\mathbf{x} - (u' - c' \mathbf{w}(\theta, \varphi))\tau, t + \Delta t - \tau, \theta, \varphi) \right] \sin \varphi d\varphi d\theta \\ &= \frac{1}{4\pi} \int_0^{2\pi} \int_0^\pi \left[(3n_1 n_2)u_Q + (3n_2^2 - 1)v_Q + 3n_2 n_3 w_Q \right] \sin \varphi d\varphi d\theta \\ & \frac{\Delta t}{4\pi} \int_0^{2\pi} \int_0^\pi \left[n_3 S(\mathbf{x} - (u' - c' \mathbf{w}(\theta, \varphi))\tau, t + \Delta t - \tau, \theta, \varphi) \right] \sin \varphi d\varphi d\theta \\ &= \frac{1}{4\pi} \int_0^{2\pi} \int_0^\pi \left[(3n_1 n_3)u_Q + 3n_2 n_3 v_Q + (3n_3^2 - 1)w_Q \right] \sin \varphi d\varphi d\theta. \end{aligned}$$

For the integrals containing p_x , p_y , p_z need to be replaced by integrals over the cone mantle. This can be done using Taylor theorem and integration by parts.

Finally, we arrive to the approximate evolution operator which called EG3.

$$\rho(P) = \rho(P') - \frac{p(P')}{c'^2} \tag{3.2.13}$$

$$+ \frac{1}{4\pi} \int_0^{2\pi} \int_0^\pi \left[\frac{p(Q)}{c'^2} - 3\frac{\rho'}{c'} n_1 u(Q) - 3\frac{\rho'}{c'} v(Q) n_2 - 3\frac{\rho'}{c'} n_3 w(Q) \right] \sin \varphi d\varphi d\theta,$$

$$u(P) = \frac{2}{3}u(P') + \tag{3.2.14}$$

$$\frac{1}{4\pi} \int_0^{2\pi} \int_0^\pi \left[-3n_1 \frac{p(Q)}{\rho' c'} + (4n_1^2 - 1)u(Q) + 4n_1 n_2 v(Q) + 4n_1 n_3 w(Q) \right] \sin \varphi d\varphi d\theta \tag{3.2.15}$$

$$v(P) = \frac{2}{3}v(P') + \frac{1}{4\pi} \int_0^{2\pi} \int_0^\pi \left[-3n_2 \frac{p(Q)}{\rho'c'} + 4n_1n_2u(Q) + (4n_2^2 - 1)v(Q) + 4n_2n_3w(Q) \right] \sin \varphi d\varphi d\theta, \quad (3.2.16)$$

$$w(P) = \frac{2}{3}w(P') + \frac{1}{4\pi} \int_0^{2\pi} \int_0^\pi \left[-3n_3 \frac{p(Q)}{\rho'c'} + 4n_1n_3u(Q) + 4n_2n_3v(Q) + (4n_3^2 - 1)w(Q) \right] \sin \varphi d\varphi d\theta, \quad (3.2.17)$$

$$p(P) = \frac{1}{4\pi} \int_0^{2\pi} \int_0^\pi \left[p(Q) - 3\rho'c'u(Q)n_1 - \rho'c'n_2v(Q) - \rho'c'n_3w(Q) \right] \sin \varphi d\varphi d\theta. \quad (3.2.18)$$

Now we reformulate the integral equations (1.39), (1.40), (1.41) for u , v , w using the second, third and fourth equation of the linearized system(2.2) we can replace integrals containing p_x , p_y , p_z and $u(P')$, $v(P')$, $w(P')$ by means of $u(P)$, $v(P)$, $w(P)$ in the following way.

Using these equations of system (2.2) we see that

$$\frac{1}{\rho'}p_x = -(u_t + u'u_x + v'u_y + w'u_z) \quad (3.2.19)$$

$$\frac{1}{\rho'}p_y = -(v_t + u'v_x + v'v_y + w'v_z) \quad (3.2.20)$$

$$\frac{1}{\rho'}p_z = -(w_t + u'w_x + v'w_y + w'w_z) \quad (3.2.21)$$

so we have

$$\frac{-1}{\rho'} \int_0^{\Delta t} p_x d\tau = \int_0^{\Delta t} (u_t + u'u_x + v'u_y + w'u_z) d\tau = u(P) - u(P') \quad (3.2.22)$$

in the same way it comes

$$\frac{-1}{\rho'} \int_0^{\Delta t} p_y d\tau = \int_0^{\Delta t} (v_t + u'v_x + v'v_y + w'v_z) d\tau = v(P) - v(P') \quad (3.2.23)$$

$$\frac{-1}{\rho'} \int_0^{\Delta t} p_z d\tau = \int_0^{\Delta t} (w_t + u'w_x + v'w_y + w'w_z) d\tau = w(P) - w(P') \quad (3.2.24)$$

depending on equations 3.2.22, 3.2.23, 3.2.24 we can simplify \tilde{S}_2 which becomes

$$\begin{aligned} \tilde{S}_2 &= \frac{\Delta t}{4\pi} \int_0^{2\pi} \int_0^\pi [n_1 S(\mathbf{x} - (u' - c'\mathbf{w}(\theta, \varphi))\tau, t + \Delta t - \tau, \theta, \varphi)] \sin \varphi d\varphi d\theta + \\ &\quad - \frac{1}{4\pi} \int_0^{2\pi} \int_0^\pi \left[p_x(x, t)(n_2^2 + n_3^2) - p_y(x, t)n_1n_2 - p_zn_1n_3 \right] \sin \varphi d\varphi d\theta + O(\Delta t^2) \\ &= \frac{\Delta t}{4\pi} \int_0^{2\pi} \int_0^\pi \left[n_1 S(\mathbf{x} - (u' - c'\mathbf{w}(\theta, \varphi))\tau, t + \Delta t - \tau, \theta, \varphi) \right] \sin \varphi d\varphi d\theta \\ &\quad + \frac{2}{3}(u(P) - u(P')) \end{aligned}$$

in the same procedure we find that

$$\begin{aligned} \tilde{S}_3 &= \frac{\Delta t}{4\pi} \int_0^{2\pi} \int_0^\pi \left[n_2 S(\mathbf{x} - (u' - c'\mathbf{w}(\theta, \varphi))\tau, t + \Delta t - \tau, \theta, \varphi) \right] \sin \varphi d\varphi d\theta \\ &\quad + \frac{2}{3}(v(P) - v(P')). \\ \tilde{S}_4 &= \frac{\Delta t}{4\pi} \int_0^{2\pi} \int_0^\pi \left[n_3 S(\mathbf{x} - (u' - c'\mathbf{w}(\theta, \varphi))\tau, t + \Delta t - \tau, \theta, \varphi) \right] \sin \varphi d\varphi d\theta \\ &\quad + \frac{2}{3}(w(P) - w(P')). \end{aligned}$$

note that \tilde{S}_1 and \tilde{S}_5 unchanged.

Now the time integral is approximated with the rectangular rule and the second part of the source terms $\tilde{S}_2, \tilde{S}_3, \tilde{S}_4$ can be evaluated using lemma (2.2.1).

So we end up with these approximate evolution operators

$$\rho(P) = \rho(P') - \frac{p(P')}{c'^2} \quad (3.2.25)$$

$$+ \frac{1}{4\pi} \int_0^{2\pi} \int_0^\pi \left[\frac{p(Q)}{c'^2} - \frac{\rho'}{c'} n_1 u(Q) - \frac{\rho'}{c'} n_2 v(Q) - \frac{\rho'}{c'} n_3 w(Q) \right] \sin \varphi d\varphi d\theta ,$$

$$u(P) = \frac{3}{4\pi} \int_0^{2\pi} \int_0^\pi \left[-n_1 \frac{p(Q)}{\rho' c'} (4n_1^2 - 1) u(Q) \right. \\ \left. + 4n_1 n_2 v(Q) + 4n_1 n_3 w(Q) \right] \sin \varphi d\varphi d\theta , \quad (3.2.26)$$

$$v(P) = \frac{1}{4\pi} \int_0^{2\pi} \int_0^\pi \left[-\frac{p(Q)}{\rho' c'} + 4n_1 n_2 u(Q) \right. \\ \left. + (4n_2^2 - 1)v(Q) + 4n_2 n_3 w(Q) \right] \sin \varphi d\varphi d\theta \quad (3.2.27)$$

$$w(P) = \frac{3}{4\pi} \int_0^{2\pi} \int_0^\pi \left[-\frac{p(Q)}{\rho' c'} + n_1 n_3 u(Q) \right. \\ \left. + n_2 n_3 v(Q) + (4n_3^2 - 1)w(Q) \right] \sin \varphi d\varphi d\theta , \quad (3.2.28)$$

$$p(P) = \frac{1}{4\pi} \int_0^{2\pi} \int_0^\pi \left[\frac{p(Q)}{c'^2} - \frac{\rho'}{c'} u(Q) \cos \theta \sin \varphi - \frac{\rho'}{c'} v(Q) \sin \theta \sin \varphi \right. \\ \left. - \frac{\rho'}{c'} w(Q) \cos \varphi \right] \sin \varphi d\varphi d\theta \quad (3.2.29)$$

3.3 Numerical Algorithms

In the case of Euler equations, we note that due to the effect of advection the center of the sonic sphere which constitutes the base of the Mach cone will not coincide with the vertex or the midpoint in the mesh. This means that any vertex or midpoint will be shifted according to local speeds. Thus in this case we need to determine the center of the sonic sphere according to the local velocities which are compared with the local speed of sound to decide the kind of the flow (sonic, supersonic, subsonic)

which will be used to determine the time step, and so we can explain that in this algorithm for the linearized Euler equations.

3.3.1 First order algorithm for the linearized Euler equations

- Input the initial data: $\rho_i^0, u_i^0, v_i^0, w_i^0, p_i^0$.
- Determine the center of the sonic sphere using the local velocities.
- Determine the time step Δt .
- Perform the time loop
 1. Determine the intermediate values: $\tilde{\rho}_{s_{ij}}^{n+\frac{1}{2}}, \tilde{u}_{s_{ij}}^{n+\frac{1}{2}}, \tilde{v}_{s_{ij}}^{n+\frac{1}{2}}, \tilde{w}_{s_{ij}}^{n+\frac{1}{2}}, \tilde{p}_{s_{ij}}^{n+\frac{1}{2}}$.
 2. Update the primitive variables.
 3. Apply the boundary conditions.
- End the time loop.

Note that in the case of linearized Euler equations, local variables are kept constant. This means that all local variables have the same value at all vertices and midpoints and this value once assigned outside the time loop does not change with time. With these known values of the local variables, it is easy to find the new centers of the bases of the Mach cones. Since local velocities are constant, the sphere position does not change with time. The determination of the time step also depends upon the local velocities i.e. $\Delta t = h_{\min} \text{CFL} / \max(|u'| + c', |v'| + c', |w'| + c')$.

Note: CFL=Courant-Friedrichs-Lewy.

The approximate evolution operators are applied at the new centers for the sonic spheres which requires the angular contribution of the neighbours at that point. The angles are therefore computed with respect to the new origin at all quadrature points. Note that taking $\rho' = c' = 1$ and neglecting the first equation in system (2.2.12) gives the advection wave equation system with propagation speed equal to 1.

$$\begin{aligned}
 p_t + (u + u' p)_x + (v + v' p)_y + (w + w' p)_z &= 0, \\
 u_t + u' u_x + v' u_y + w' u_z + p_x &= 0, \\
 v_t + u' v_x + v' v_y + w' v_z + p_y &= 0, \\
 w_t + u' w_x + v' w_y + w' w_z + p_z &= 0.
 \end{aligned} \tag{3.3.30}$$

3.3.2 EG Schemes for Nonlinear Euler Equations

The FVEG schemes that have been established in Section 3.2 for the linearized Euler equations are now extended to the solution of the non-linear Euler equations. In the linearization process we have treated the non-linear Euler equations by considering small perturbations in density (ρ), velocities (u, v, w), sound speed (c) and pressure (p). Example 4.1.2 for the linearized Euler equations that follows below demonstrates the propagation of acoustic, entropy and vorticity pulses along the diagonal of the mesh. In that case the local variables stayed constant at all points of the mesh and for all time steps. This introduces a considerable simplification to the non-linear phenomena and hence contributes to the error in evaluation of the physical quantities like density, velocities and pressure. Many numerical schemes treating non-linear Euler equations carry out no linearization for example kinetic schemes, central type schemes,

Godunov type upwind schemes and many others. However EG and FVEG schemes do need some kind of linearization at an early stage. In this section we shall use the same approximate evolution operators as we used for linearized Euler equations, however the local variables will have different values at different quadrature points. This means that each vertex and midpoint of an edge will have a particular value which will be different than the other points. These values will be calculated by an appropriate averaging procedure at these points. In the next time steps these variables will have to be recalculated at all points. In this way the updated values of the physical quantities are involved in the calculation of local variables at each time step which brings the non-linear effects into play.

Now due to the effect of advection the center of the sonic sphere which constitutes the base of the Mach cone does not coincide with a vertex or a midpoint in the mesh. This means that any vertex or midpoint will be shifted according to local speeds. Thus the first order algorithm for non-linear Euler equations reads

- Input the initial data: $\rho_i^0, u_i^0, v_i^0, w_i^0, p_i^0$.
- Compute the conservative variables.
- Find the center of the sonic sphere using the the initial local variables
- Find the initial time step
- Perform the time loop
 1. Find the local variables: ρ', u', v', w', p' at all quadrature points.

2. Find the centres of the sonic spheres using the local velocities.
 3. Find the global maximum of $(|u'| + c', |v'| + c', |w'| + c')$.
 4. Find the time step $\Delta t = \frac{(h_{\min})(\text{CFL})}{\max(|u'| + c', |v'| + c', |w'| + c')}$.
 5. Compute the intermediate values: $\tilde{\rho}_{s_{i_j}}^{n+\frac{1}{2}}, \tilde{u}_{s_{i_j}}^{n+\frac{1}{2}}, \tilde{v}_{s_{i_j}}^{n+\frac{1}{2}}, \tilde{w}_{s_{i_j}}^{n+\frac{1}{2}}, \tilde{p}_{s_{i_j}}^{n+\frac{1}{2}}$.
 6. Update the conservative variables:
 7. Compute the primitive variables.
 8. Apply the boundary conditions.
- End the time loop.

Chapter 4

Numerical Experiments

In this chapter we will consider three numerical experiments in each we will consider two cases subsonic and supersonic, and we will try to make comparison between the two cases in each experiment.

4.1 Linearized Euler

Example 4.1.1

In this experiment we consider the advection wave equation system with the following initial data is considered

$$\begin{aligned} p(x, y, z, 0) &= -(\sin(2\pi x) + \sin(2\pi y) + \sin(2\pi z)), \\ u(x, y, z, 0) &= 0, \\ v(x, y, z, 0) &= 0, \\ w(x, y, z, 0) &= 0. \end{aligned}$$

The exact solution is

$$\begin{aligned}
 p(x, y, z, t) &= -\cos(2\pi t)(\sin 2\pi(x - u't) + \sin 2\pi(y - v't) + \sin 2\pi(z - w't)), \\
 u(x, y, z, t) &= \sin(2\pi t) \cos 2\pi(x - u't), \\
 v(x, y, z, t) &= \sin(2\pi t) \cos 2\pi(y - v't), \\
 w(x, y, z, t) &= \sin(2\pi t) \cos 2\pi(y - w't).
 \end{aligned}$$

For the subsonic case we take $u' = v' = w' = 0.5$ together with $\text{CFL} = 0.5$, with absolute time 0.1. The computational domain is $\Omega = [-1, 1] \times [-1, 1] \times [-1, 1]$. In Table 4.1 we present the L^2 -error results for FVEG-Euler-3D-N1 scheme, where the experimental order of convergence (EOC) = $\ln \frac{\|\mathbf{U}_{N_1}(T) - \mathbf{U}_{N_1}^n\|}{\|\mathbf{U}_{N_2}(T) - \mathbf{U}_{N_2}^n\|} / \ln(N_2/N_1)$, where N_1, N_2 represents the number of cells in two meshes. Notice that in this table N is the total number of cells in the mesh. Furthermore for this experiment we implement exact boundary conditions.

N	$\ p(T) - p^n\ $	$\ u(T) - u^n\ $	$\ \mathbf{U}(T) - \mathbf{U}^n\ $	EOC
20	0.098602327828	0.123327159725	0.23531938789	-
40	0.061987721507	0.062560020999	0.12477091188	0.9153
80	0.035460387807	0.032162217244	0.06595525974	0.9197
160	0.019028736560	0.016923319531	0.03492416386	0.9173

Table 4.1: Advection equation-(subsonic case), FVEG-N1 scheme, T=0.1, CFL=0.5

Comparison between the exact solution and the approximated solution for the first order scheme is shown in Figures 4.1, 4.2. These are 1D plots along the line $y = 0$. The plots show that the numerical solution is in good agreement with the exact solution. We see that by increasing the mesh size that L^2 error becomes

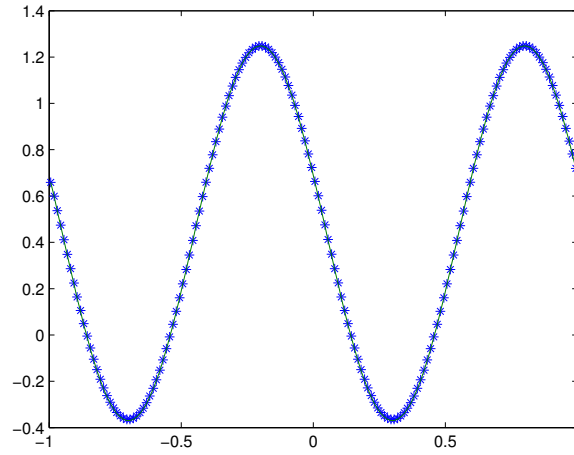


Figure 4.1: Advection equation-(subsonic case),FVEG-N1 scheme, $T=0.1$, $CFL=0.5$, $P(x,0,0)$ $N=160$, *:numerical solution,- : exact solution

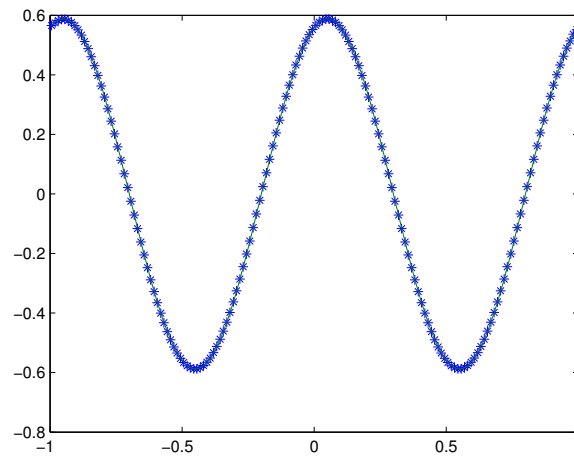


Figure 4.2: Advection equation-(subsonic case),FVEG-N1 scheme, $T=0.1$, $CFL=0.5$ $u(x,0,0)$, $N=160$, *:numerical solution, -: exact solution

more smaller and so the numerical solution becomes more close to the exact solution.

The second part of the example is the supersonic case, here we take $u' = v' = w' = 0.8$ together with $\text{CFL} = 0.5$, also with absolute time 0.1. The computational domain is $\Omega = [-1, 1] \times [-1, 1] \times [-1, 1]$. In Table 4.2 we present the L^2 -error results for N1-Euler-3D scheme. Where N here is the total numbers of cells in the mesh. Furthermore for this experiment we implement exact boundary conditions. Comparison between the exact solution and the approximated solution for the first order scheme is shown in Figures 4.3, 4.4. It is like the subsonic case, the increasing of mesh size the decreasing of the L2-error but here we see that the decreasing in the error is not as that in the subsonic case. These are 1D plots along the line $y = 0$.

N	$\ p(T) - p^n\ $	$\ u(T) - u^n\ $	$\ \mathbf{U}(T) - \mathbf{U}^n\ $	EOC
20	0.160592582154	0.108937141433	0.24778770616	-
40	0.092666380757	0.056451512259	0.13461335430	0.8803
80	0.050714556878	0.030029307768	0.07244306802	0.8939
160	0.026651269471	0.016565522521	0.03888862611	0.8975

Table 4.2: FVEG-N1 scheme, advection equation-(supersonic case), T=0.1, CFL=0.5

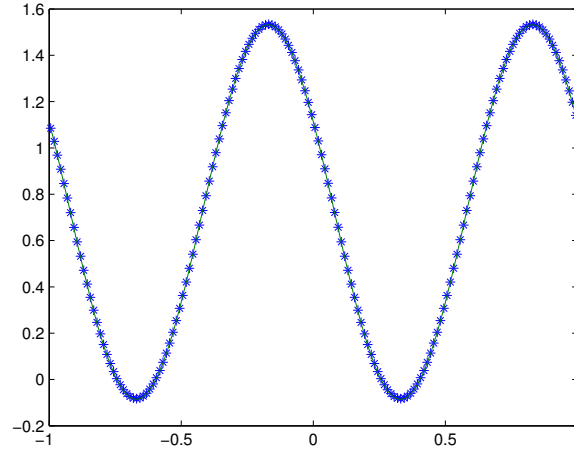


Figure 4.3: FVEG-N1 scheme, advection equation (supersonic case), $T=0.1$, $CFL=0.5$ $p(x,0,0)$, $N = 160$, *:numerical solution, -: exact solution

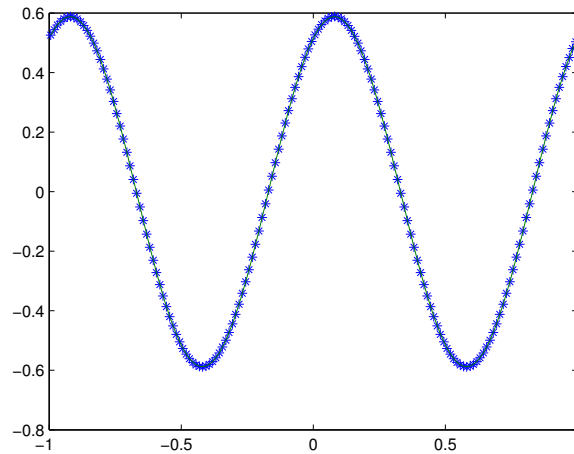


Figure 4.4: FVEG-N1 scheme, advection equation (supersonic case), $u(x,0,0)$, $T=0.1$, $CFL=0.5$, $N=160$ *:numerical solution, -: exact solution

Example 4.1.2

In this experiment we simulate numerically the propagation of acoustic pulse in a uniform mean flow propagating along the x -axis. The linearized Euler equations system (2.2.8) has been considered together with the following initial data.

$$\begin{aligned}\varphi(x, y, z, 0) &= 1 + \frac{2.5}{40\sqrt{8}} \exp(-40(x^2 + y^2 + z^2)), \\ u(x, y, z, 0) &= 0.5, \\ v(x, y, z, 0) &= 0.0, \\ w(x, y, z, 0) &= 0.0, \\ p(x, y, z, 0) &= \frac{1}{\gamma} + \frac{2.5}{40\sqrt{8}} \exp(-40(x^2 + y^2 + z^2)).\end{aligned}$$

Assume $u' = 0.5$ and $v' = w' = 0$, which means that the local flow is subsonic. Initially, the acoustic pulse is generated at $(0, 0, 0)$. The mean flow interacts with this pulse. The intensity, shape and profile of the propagating waves are also affected by the mean flow. We consider CFL=0.5 and the mesh is consisting of 40, 80 and 160 cells where the extrapolated boundary conditions are employed. We examine the propagation of the pulses after time $T = 0.5$. We plot the pressure p along the line $y = 0$ and compare the first order FVEG-Euler-3D scheme(N1) with the exact solution the numerical solution is in very good agreement with the exact solution.

For the supersonic case we assume that the local flow is along the x axis with $u' = 1.1$ and the CFL =0.5 and as in the subsonic case we take mesh consisting of 40,80, 160 cells with absolute time 0.5. in the graph below we can see that the numerical solution also in good agreement with the exact solution.

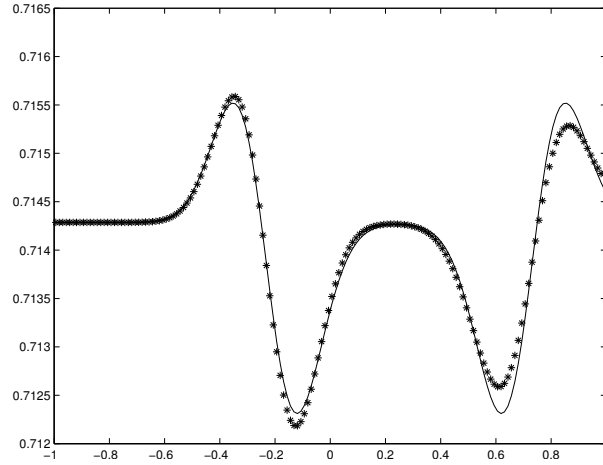


Figure 4.5: FVEG-N1 scheme, acoustic pulse-subsonic case, $T=0.5$, $CFL=0.5$

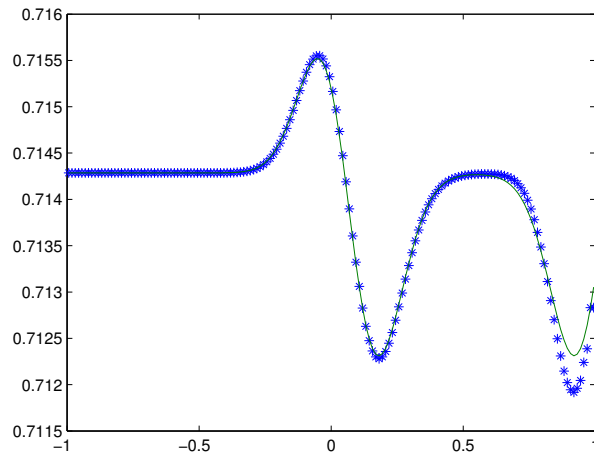


Figure 4.6: FVEG-N1 scheme, acoustic pulse-supersonic case, $T=0.5$, $CFL=0.5$

4.2 Non-linear Euler

Example 4.2.1

We consider non-linear Euler equations and a spherical explosion problem in a cubic domain $\Omega = [-1, 1] \times [-1, 1] \times [-1, 1]$ as shown in Figure 4.7. the following initial data is considered

$$(\rho, u, v, w, p) = \begin{cases} (1, 0, 0, 0, 1) & \text{if } (x^2 + y^2 + z^2) < 0.16 \\ (0.125, 0, 0, 0, 0.1) & \text{otherwise.} \end{cases}$$

The pressure and density inside the spherical region of radius 0.4 is greater than that in the outside region. This pressure difference generates a shock wave expanding towards the boundary of the domain. A contact discontinuity moves along with the shock while a spherical rarefaction wave travels towards the origin at $(0,0,0)$. In graph (4.2) we see density distribution as a function of x and y on the plane $z=0$ at time $t=0.1$. Figure (4.2) we see the corresponding pressure distribution on the plane $z=0$. Figures(4.2, 4.2) represents the density, and the pressure distribution on the xy plane compared with the same variables for the equivalent problem in the one dimensional case. Note that in this experiment we use $CFL = 0.5$ and mesh size is $80 \times 80 \times 80$, and absolute time 0.1 .

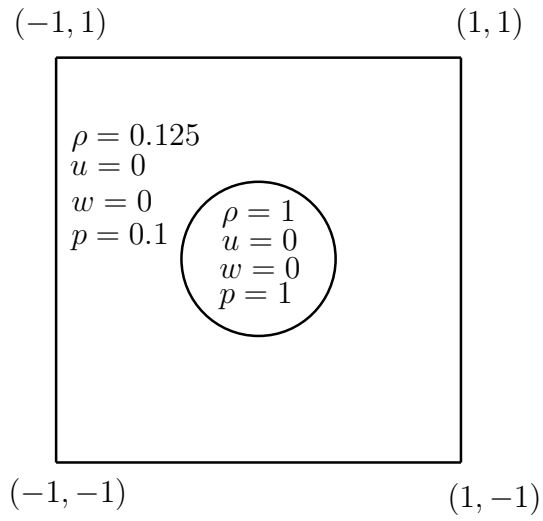


Figure 4.7: Domain for the spherical explosion problem

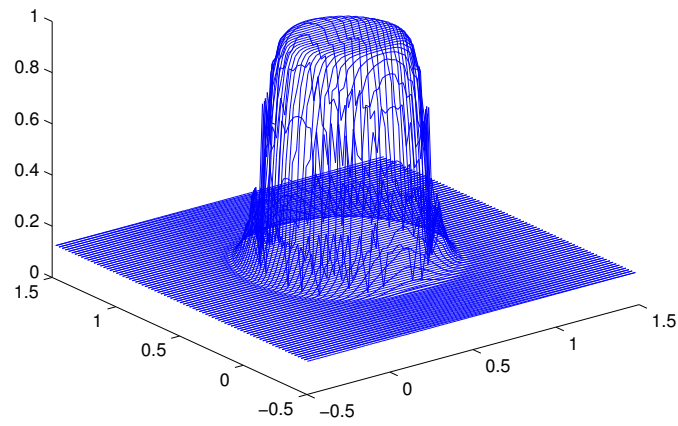


Figure 4.8: spherical explosion. Density distribution at $t=0.1$.

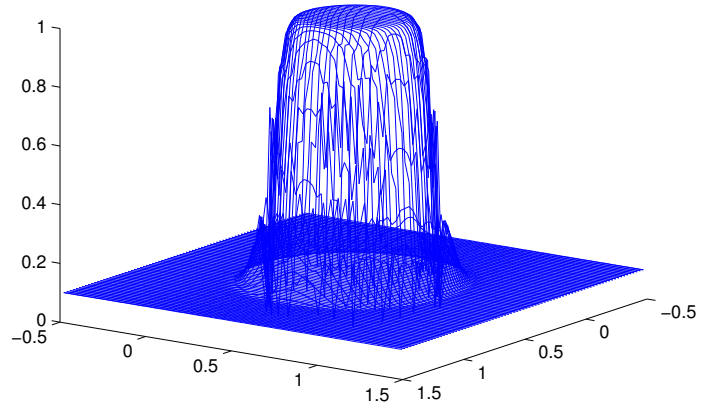


Figure 4.9: spherical explosion. Pressure distribution at time $t=0.1$.

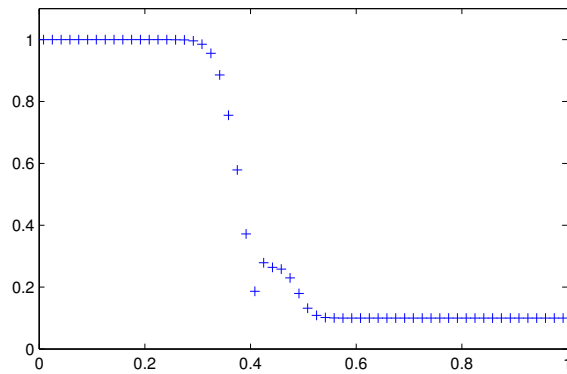


Figure 4.10: FVEG-Euler-3D-N1 scheme, 1D distribution of pressure

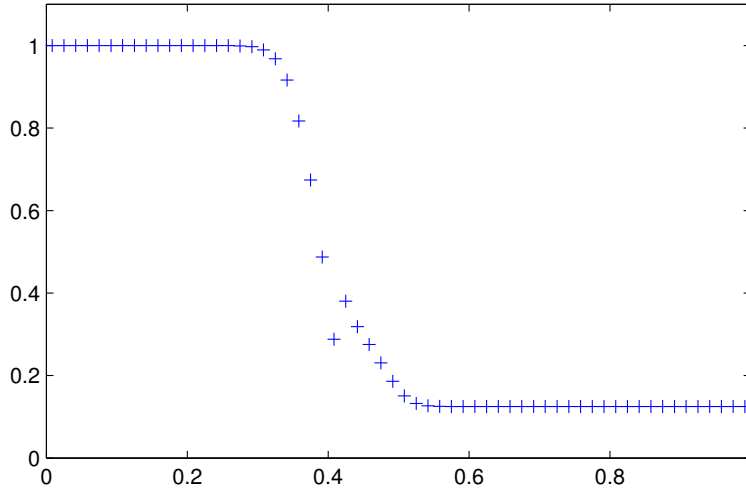


Figure 4.11: FVEG-N1 scheme, 1D distribution of density

4.3 Conclusion and Outlook

The main aim of this thesis was to solve three dimensional Euler equations system using Evolution Galerkin method. In chapter 2 the general theory of linear hyperbolic systems of partial differential equations have been used to derive the exact integral equations for the linearized system. And in chapter 3 we derived three approximate evolution operators for the system namely(N1,EG1,EG3). These operators have been tested extensively on a different numerical experiments in chapter 4 where we see in these experiments the accuracy and the multidimensional behaviour of the solution.

In this thesis we have tested a first order scheme for the three dimensional Euler equations system, were a second order scheme can be derived using a suitable recovery stage which well be our next aim in the future.

Bibliography

- [1] Z-C. Zhang and S.-T. John Yu, A generalized space-time CE/SE method for the Euler equations on quadrilateral and hexagonal meshes, AIAA 2001-2592, (2001).
- [2] S. Billet, E.F. Toro. On WAF-type schemes for multidimensional hyperbolic conservation laws. *J. Comput. Phys.*, 130:1-24, 1997.
- [3] L. C. Evans. *Partial Differential Equations*. American Mathematical Society, 1998.
- [4] T. Kröger, M. Lukáčová-Medvidová. An evolution Galerkin scheme for the shallow water magnetohydrodynamic (SMHD) equations in two space dimensions. *J. Comp. Phys.*, 206:122-149, 2005.
- [5] P. Lin, K.W. Morton and E. Süli. Characteristic Galerkin schemes for scalar conservation laws in two and three space dimensions. *SIAM J. Numer. Anal.*, 34(2):779–796, 1997.
- [6] P. Lin, K.W. Morton and E. Süli. Euler characteristic Galerkin scheme with recovery. *M²AN*, 27(7):863–894, 1993.
- [7] R.J. LeVeque. Wave propagation algorithms for multi-dimensional hyperbolic systems. *J. Comp. Phys.*, 131:327-353, 1997.
- [8] M. Lukáčová-Medvidová, K. W. Morton and G. Warnecke. Finite volume evolution Galerkin methods for Euler equations of gas dynamics. *Int. J. Num. Methods in Fluids*, 40(3-4):425–434, 2002.
- [9] M. Lukáčová-Medvidová, K. W. Morton and G. Warnecke. Finite volume evolution Galerkin FVEG methods for hyperbolic systems. *SIAM J. Sci. Comp.*, 26(1):1–30, 2004.

- [10] M. Lukáčová-Medvidová, K.W. Morton and G. Warnecke. High resolution finite volume evolution Galerkin schemes for multidimensional conservation laws. Proceedings of ENUMATH'99, World Scientific Publishing Company, Singapore, 1999.
- [11] M. Lukáčová-Medvidová, K.W. Morton and G. Warnecke. Evolution Galerkin methods for hyperbolic systems in two space dimensions. *Math. Comput.*, 69(232):1355–1384, 2000.
- [12] M. Lukáčová-Medvidová, K.W. Morton, and G. Warnecke. Evolution Galerkin methods for multidimensional hyperbolic systems. Proceedings of ECCOMAS 2000, Barcelona, 1-14, 2000.
- [13] M. Lukáčová-Medvidová, J. Saibertová and G. Warnecke. Finite volume evolution Galerkin methods for nonlinear hyperbolic systems. *J. Comput. Phys.*, 183:533–562, 2002.
- [14] M. Lukáčová-Medvidová, J. Saibertová, G. Warnecke and Y. Zahaykah. On evolution Galerkin methods for the Maxwell and the linearized Euler equations. *Appl. Math.*, 49(5):415–439, 2004.
- [15] M. Lukáčová-Medvidová, G. Warnecke, and Y. Zahaykah. Third order finite volume evolution Galerkin (FVEG) methods for two-dimensional wave equation system. *J. Numer. Math.*, 11(3):235–251, 2003.
- [16] M. Lukáčová-Medvidová, G. Warnecke and Y. Zahaykah. On the stability of the evolution Galerkin schemes applied to a two-dimensional wave equation system. *SIAM J. Numer. Anal.*, 2005.
- [17] S. Noelle. The MOT-ICE: a new high-resolution wave-propagation algorithm for multi-dimensional systems of conservative laws based on Fey's method of transport. *J. Comput. Phys.*, 164:283-334, 2000.
- [18] S. Ostkamp. Multidimensional characteristic Galerkin schemes and evolution operators for hyperbolic systems. *Math. Meth. Appl. Sci.*, 20:1111–1125, 1997.
- [19] Y. Zahaykah. *Evolution Galerkin Schemes and Discrete Boundary Conditions for Multidimensional First Order Systems*. Dissertation, Magdeburg, 2002.

- [20] E.F. Toro, Riemann solvers and numerical method for fluid dynamics, Second Edition, Springer-Verlag, New York, (1995).
- [21] Randall J. Leveque, Finite Volume Methods for Hyperbolic Problems, Second Edition, Cambridge University, (2004).
- [22] Nesayahu, H. Tadmor, E. Non oscillatory Central differencing for hyperbolic conservation laws *J. Comput. phys*, 87: 408—463, (1990)